Production of furfural: From kinetics to process assessment

Daniel Edumujeze, Marie-Christine Fournier-Salaün, Sébastien Leveneur

Fuel 381 (2025) 133423

Contents lists available at ScienceDirect

Fuel

journal homepage: www.elsevier.com/locate/fuel

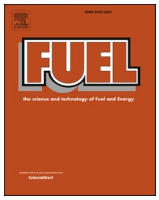

Review article

Production of furfural: From kinetics to process assessment

Daniel Edumujeze, Marie-Christine Fournier-Salaün, Sebastien Leveneur *

INSA Rouen Normandie, Univ Rouen Normandie, Normandie Univ, LSPC UR 4704, F-76000 Rouen, France

ARTICLE INFO

Keywords:
Furfural
Kinetic modeling
Purification
Solvent screening

ABSTRACT

The valorization of lignocellulosic biomass from waste into high-value-added molecules has gained tremendous attention due to its availability and non-competition with food. Furfural, a prominent platform molecule is exclusively derived from lignocellulosic biomass and a promising platform for biofuels. Existing literature provides numerous reviews on furfural production, focusing on the catalyst and solvent effects. There is a notable gap concerning its kinetics and overall process assessment. To address this, we investigated different lignocellulosic biomass pretreatment methods while considering their economic and environmental implications from a process assessment and sustainability standpoint. Within the framework of this review, recent progress in the production of furfural was discussed while considering the effects of catalysts, solvents, and operating conditions. Furthermore, the reaction pathways and kinetic models proposed for furfural production both directly from lignocellulosic biomass and xylose were discussed. Additionally, recent and innovative process intensification and purification technologies for furfural were examined. Finally, we proposed a sustainable process for obtaining furfural directly from lignocellulosic biomass which can be easily implemented in an industrial scale setting while abiding by the green chemistry principles. This review consolidates current knowledge on furfural production, integrates critical aspects often overlooked in previous studies, and outlines a pathway toward a robust and environmentally sound industrial process for furfural synthesis from renewable biomass sources.

1. Introduction

Transitioning from dependency on fossil sources such as coal, natural gas, and petroleum to using renewable sources to meet our basic energy and chemical needs has been the most intense and debated discussion within the European Union and the world. Our dependency on fossil fuels has led to ever-increasing health, environmental, and climate issues. On a global scale, fossil fuel contributes to about 79 % of greenhouse gas emissions. The last five years have been the most extreme on record, with total energy-related CO_2 emissions reaching a new all-time high of 37.4 Gt/year [1]. To achieve the ambitious target set by the European Commission during the Paris Agreement and its goals to mitigate greenhouse gas emissions by 55 % on or before 2050, the transition from fossil to renewable sources must be swift and sustainable.

Amidst other renewable energy sources such as wind, solar, hydro, geothermal, biomass, etc., lignocellulosic biomass (LCB) has the highest potential of abating greenhouse gas emissions since it is the only carbon-fixing renewable energy source. It is particularly abundant, relatively cheap, and has the potential to be transformed into high-value bio-based chemicals. Besides, one can select several LCB materials that do not compete with the food sector such as agricultural waste, dedicated crops, etc. These bio-based chemicals and platform molecules from lignocellulosic biomass could be a sustainable replacement for the fossil counterpart and a possible solution to our dependency on fossil molecules.

Lignocellulosic biomass typically comprises about 35–50 % cellulose, 20–35 % hemicellulose, and 10 – 25 % lignin depending on its sources, species of the plant, growth conditions, and region of cultivation [2]. With the right approach, these fractional constituents of LCB can be sustainably transformed into a spectrum of high-value and marketable products that can serve as sustainable alternatives to the fossil-based counterpart while adhering to green chemistry principles. The concept of a lignocellulosic biorefinery becomes admirable as it utilizes readily available and non-edible biomass that does not compete with food, land, and water to produce a spectrum of valuable products [3]. Similar to the petroleum refinery, the lignocellulosic biorefinery can utilize the entire LCB component to produce desirable products. However, the abundant oxygen-containing functional groups present in the molecular structure of lignocellulosic biomass such as hydroxyl (—OH),

* Corresponding author.
E-mail address: sebastien.leveneur@insa-rouen.fr (S. Leveneur).

https://doi.org/10.1016/j.fuel.2024.133423
Received 18 July 2024; Received in revised form 6 October 2024; Accepted 10 October 2024
Available online 15 October 2024

acetyl (—$OCOCH_3$), methoxy (—OCH_3), carboxyl (—COOH), ether (—C—O—O), phenolic hydroxyl (—OH), carbonyl group (—C═O), etc reduces its energy density when compared to the fossil counterpart [4–6]. As such, it is crucial to either reduce the excess oxygen molecules to improve their energy density for biofuel production or transform them into molecules with diverse functional groups that are pivotal for industrial applications. Through the integration of sustainable green chemistry principles and a biorefinery approach, the LCB can be transformed via thermochemical (combustion, liquefaction, pyrolysis, and gasification), biological (microbial processing, digestion, and fermentation) or chemical routes (dehydration, hydrogenation, etc) as illustrated in Fig. 1.

Although the valorization of lignocellulosic biomass has been advocated as a sustainable alternative to its fossil counterpart, its full commercialization is limited by several economic, social, environmental, political, and technological constraints [7]. The development of a dependable and cost-effective logistics network and supply chain are critical phases toward the commercialization of the LCB valorization processes. Biomass logistics and transportation improvements are necessary for lignocellulosic biorefineries to become feasible, as they currently lack operational viability [8].

Additionally, the search for effective catalysts is still one of the major challenges as the composition of the feedstocks (LCB), the reaction pathways, and operating conditions are completely different from those of well-established petroleum processes.

While petroleum and petrochemical processes mainly occur at high temperatures (> 400 °C) and through the vapor phase, lignocellulosic biomass valorization is characterized by low temperature (<300 °C) liquid phase reaction pathways such as hydrolysis, dehydration, isomerization, oxidation, aldol condensation, hydrogenation, fermentation, and transesterification [10]. For such reactions, the catalyst must be specifically designed to resist in situ leaching during the process, be hydrothermally stable over a wide range of pH, and have a tuneable hydrophobicity. Additionally, careful manipulation of catalyst pore sizes and structures during their design is essential to overcome mass transport limitations.

While it is essential to scale-up the production process to meet the energy and chemical demands, it can be challenging as the optimized conditions and process strategies developed for the experimental and pilot stages may not show similar performance indices during scale-up [11]. The development and assessment of robust and well-detailed kinetic and thermodynamic models become essential for tackling technological challenges involved with scaling up lignocellulosic valorization processes. When targeting high-valued and marketable molecules that can only be obtained from the valorization of lignocellulosic biomass, accurate development and prediction of the model's constants are particularly crucial. With the aid of a well-developed and optimized model, it becomes possible to profitably obtain these molecules on a commercialized scale, thus enhancing the viability of lignocellulosic biomass valorization processes.

Amongst other molecules that can be obtained from the valorization of lignocellulosic biomass, furfural has been ranked as one of the top 30 high-valued and marketable building blocks by the National Renewable Energy Laboratory [12]. Its dual functional groups contribute to its unique chemical properties and reactivity, making it a versatile molecule for diverse industrial applications [13]. The presence of the aldehyde and furan ring system makes it possible to participate in numerous reactions such as hydrogenation, oxidation, acetylation acylation, decarboxylation, aldol-condensation, etc [14,15].

The global market value of furfural reached US $520 million in 2021. It is expected to grow at a compound annual growth of approximately 5.6 % from 2022 to 2030. The IMARC group expects its market value to reach US $817.8 million by the end of 2031 [1]. Among the main reasons propelling the market are the growing need for fragrances and perfumes, increased use in the food, chemical, and pharmaceutical industries, and growing environmental concerns. The market is expected to expand further due to the increased demand for furfural alcohol (a derivative of furfural) and rising concerns about Petro-based products and transitioning into bio-based products [16].

Furfural and its derivatives are widely used as solvents,

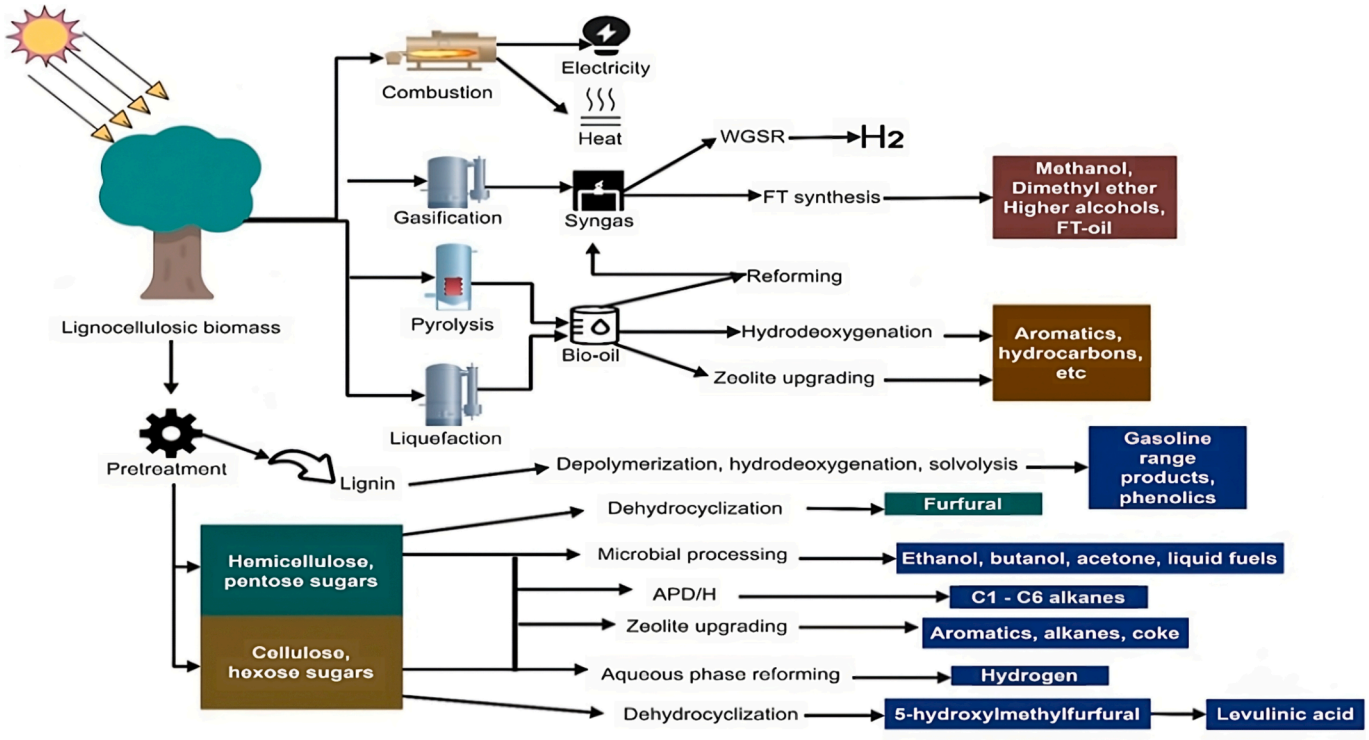

Fig. 1. Lignocellulosic biorefinery platform adapted from [9].

transportation fuels, gasoline additives, lubricants, resins, addictive, decolorizing agents, and flavor enhancers for food and drink [17]. In the field of biofuels and fuel-additives, furfural can be used to produce 2-methylfuran, 2-methyltetrahydrofuran, furfuryl alcohol, tetrahydrofurfuryl alcohol, furan, tetrahydrofuran, and various *cyclo*-products [14].

Commercially, Furfural is exclusively produced from the mineral acid hydrolysis of pentosans in lignocellulosic biomass followed by subsequent dehydration of the released pentosan sugars [18]. The furfural production process starts with the selective fractionation/pre-treatment of lignocellulosic biomass into hemicellulose, followed by hydrolysis of the hemicellulose into C-5 sugars, and finally, dehydration of the C-5 sugars to furfural. The pre-treatment processes are discussed in the subsequent section. Low product yield (<50 %), relatively high concentration of mineral acid, corrosion of equipment, and high cost of product separation and purification are some problems associated with the existing industrial production process of furfural [19]. Due to side degradationreactions occurring concurrently (condensation, fragmentation, and resinification), different strategies have been proposed in the literature ranging from the use of heterogeneous catalysts to the application of a biphasic solvent system with a singular aim of improving its yield [13,18–20]. In comparison with furfural, 5-hydroxymethylfurfural (HMF), derived from the acid dehydrocyclization of cellulose – the most abundant polymer from LCB – has been the focus of significant research due to its application in biofuels and value-added chemicals [21]. However, the development of an effective and environmental technology that can convert hemicellulose to furfural will present a great opportunity for the establishment of a sustainable lignocellulosic biorefinery.

This review focuses on providing a comprehensive and comparative investigation of the recent research on catalyst and solvent, the intensification technology for this reaction, reaction mechanisms/pathways, kinetic studies, the process flow diagrams, and the environmental impacts involved in the production of furfural found in the literature. By systematically evaluating these findings, it will be possible for industrial experts and researchers to extract insight into different and efficient modeling approaches and identify and obtain useful operating conditions for process intensification and optimization thus making it feasible to implement academic research into industrial settings.

2. Furfural production

Furfural is produced industrially via aqueous mineral acid hydrolysis of pentosans present in lignocellulosic biomass such as oat hull, corn cobs, hardwood, bagasse, etc, and the subsequent dehydration of the released pentose sugars [18]. The hydrolysis step proceeds rapidly with a high hydrolysate yield while the subsequent dehydration step is generally regarded as rate limiting, being hindered by competitive side degradation reactions such as the condensation between xylose or intermediates and furfural, fragmentation of intermediates, resinification and decomposition of furfural which subsequently leads to low product yield [22,23]. Fig. 2 presents the synthesis of furfural directly from hemicellulose. Condensation and resinification have been reported to be the two main side degradation reactions contributing to low furfural yield [23,24].

The Quaker Oats batch process is the first commercialized furfural production process from lignocellulosic biomass. It involves the mineral acid-catalyzed (H_2SO_4) hydrolysis of dry oat hull to release pentoses, followed by subsequent dehydration to furfural under a pressure of 5 atm at 153 °C for 5 h in a rotary reactor made of carbon brick lined with acid-resistant cement. The produced furfural is extracted and purified from the reactive acid residue via steam stripping and azeotropic distillation respectively. The technology is however characterized as energy intensive, time consuming, and low efficiency as the furural yield falls within 40 – 52 %. The Quaker Oats batch process was subsequently modified to a continuous process. In this case, wet bagasse is loaded into a horizontal line bricked reactor equipped with paddles to improve mass transfer. Superheated steam of 650 °C is injected in multiple locations along the reactor to supply the energy needed for pentoses dehydration at 184 °C. While the continuous process was able to reduce the reaction time by fivefold, the furfural yield remained the same.

Another significant industrial process for furfural production is the Rosenlew process. This process is notable as it does not employ external acid catalyst addition. Instead, the biomass provides the necessary catalytic environment during its degradation. This process employs a vertical-type column reactor which allows biomass to be charged from the top of the reactor through an intermittently opening shutter along a counter-current flow of 10 bar of steam At high reaction temperatures, acetic acid and formic acid are produced which autocatalytically promote biomass degradation, generating a relatively high furfural yield of 59.5 %. However, it requires a high amount of steam making the process energy-intensive.

Leveraging on these advancements, the Biofine process presents yet another approach to furfural production. Originally designed to produce levulinic acid in a multi-stage continuous process, furfural is co-produced as a byproduct during the Biofine process. In the first sage, the lignocellulosic biomass is subjected to acid degradation in a tubular reactor operating at 210 – 250 °C. To obtain a significant yield of furfural (55 wt%), 25 bar of steam is injected for 1 min without significant axial mixing. The second stage consists of a perfectly stirred reactor, which operates in a condition that allows furfural to be maintained in the vapor phase, simplifying the separation process. While the Biofine process has been optimized for high furfural yield (70 %), the need for high-pressure steam and operational cost for managing the multi-reactors remains a major drawback. Other significant industrial processes for furfural production are summarised in Table 1.

Current industrial furfural production processes are limited by low product yield, high operational cost, difficulties in product separation and purification, corrosion of equipment, and lack of catalyst reusability due to the application of homogeneous mineral acids such as H2SO4, H_3PO_4, HCl, etc. [20,25–27]. Over the past decades, several studies have been focusing on mitigating these industrial drawbacks while enhancing

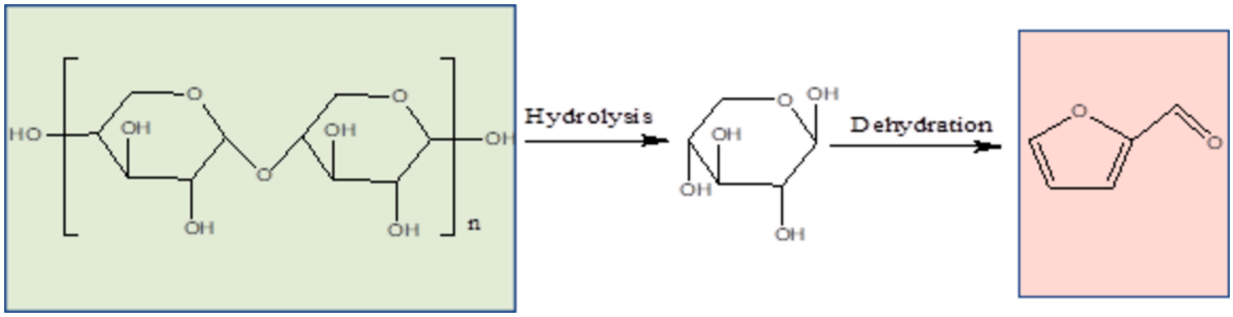

Fig. 2. Synthesis of furfural directly from hemicellulose using xylan as a model.

Table 1
Summary of key industrial furfural production technologies [23].

Technology	Operating condition	Biomass	Catalyst	Operating temperature (°C)	Furfural yield (%)
Quaker Oats	Batch	Oat hull	H_2SO_4	153	40 – 52
Chinese batch	Batch	Corn cob	H_2SO_4	160–165	50
Quaker Oats	Continuous	Bagasse	H_2SO_4	184	55
Westpro/Huaxia	Continuous	Various LCB	H_2SO_4	160–165	35 – 50
Rosenlew	Continuous	Bagasse	Autocatalysis	180	59.5
SupraYield	Continuous	N/A	H_3PO_4	180–240	50 – 50
Multi-Turbine-Column (MTC)	Continuous	Straw	H_2SO_4	180	86[a]
Vedernikovs	Continuous	Birchwood sawdust	H_2SO_4	188	75
Biofine	Continuous	Ground hardwood, paper sludge	H_2SO_4	Reactor 1: 210–220 Reactor 2: 190–200	70

[a] Including furfural and furfural alcohol.

the efficiency and sustainability of the process. More recently, heterogeneous catalyst use has gained increasing attention as they enable easier product/catalyst separation and purification, reduce equipment corrosion, and possess the potential to be used repeatedly [23]. Also, the possibility of fine-tuning their catalytic properties such as surface area, particle size, support structure, hydrophobicity, thermal stability, acidity, etc makes them even more desirable. Solid acid catalysts such as zeolites, ion exchange resins, clays, heteropoly acids, metallic oxides, and mixed oxides have been reported to be effective in producing furfural.

2.1. Catalyst effect

2.1.1. Zeolite

The wide range of applications of zeolites as catalysts for the valorization of lignocellulosic biomass can be attributed to their microporous framework, high porosity, precise pore sizes (0.4 – 1 nm), tuneable acidity, and combined with the possibility of loading them with exchangeable cations [28]. Due to their shape selectivity, zeolites can limit the formation of products larger than their pore sizes [29]. For the first time, Bruce et al. demonstrated the possibility of obtaining a furfural yield of up to 31 % using a small pore zeolite directly from pure biomass (switchgrass) without any pretreatment [30]. The low furfural yield was a result of zeolite's pore size (SAPO-34) which was significantly smaller than the kinetic diameter of sugars. However, the catalyst was recycled multiple times (3) with only a 5 % drop in furfural yield and no significant leaching of the acid sites was observed. Song et al. presented a promising protocol that led to a furfural yield of 93.6 and 85.9 % using xylose and xylan as substrates respectively in pure 1,4-dioxane and commercial H-β zeolite as catalyst [31]. The high furfural yield was attributed to the synergistic interaction between the multiple immobilized acid sites of H-β and 1,4-dioxane which accelerated xylose-xylulose isomerization. When the spent H-β zeolite was directly loaded in a new catalytic system, a significant decrease in the furfural yield (61.2 %) was observed after five successive runs, revealing significant deactivation of the catalyst.

The Si/Al ratio which directly indicates the density of Brønsted acid sites influences the overall catalytic activity and ultimately, furfural yield. Additionally, a decrease in the furfural yield due to a corresponding increase in the Si: Al ratio was reported as follows: Hβ(30) – 93.6 % > Hβ(40) – 88.3 % > Hβ(25) – 80.6 %. In another study, Gupta et al. were able to increase the acid density of H-β by grafting the sulphonic acid group (SO_3-H) to the zeolite which led to an increase in the furfural yield of 76 % [32]. The reusability study confirms that there was a marginal drop of 25 % in furfural yield after 3 recycle times. While the acid sites of zeolites are located within the core of the micropores,substrates must overcome transport limitations to access these active acid sites for effective conversion. The micropore diffusion limitations are significantly prominent in small and medium pore zeolites [33]. More recently, Wang et al. showed that modifying a H-Y zeolite via dealumination with Cr^{3+} can impact it with a rich secondary pore structure and suitable acid center density [34]. This allows furfural to rapidly leave the inner surface of the modified zeolite, thus avoiding degradation and ultimately providing a higher yield (99.7 %) at a shorter reaction time (30 min). After five successive cycles, the furfural yield decreases to some extent but remains at or above 66.1 %. Directly from lignocellulosic biomass or xylose, pure zeolites or in their modified forms are instrumental for furfural production, although the pore size, specific surface area, and Si/Al are essential factors to be considered during their design and selection.

2.1.2. Ion exchange resins

Similar to the use of zeolites, ion exchange resins have been reported to be effective for furfural synthesis. Sato et al. showed that xylose can be effectively dehydrated by Amberlyst-70 at 150 °C in a semi-batch reactor with a continuous CO_2 flow [35]. Le Guenic et al. presented a report where 80 % furfural yield was obtained from xylose dehydration by Nafion NR-50 in a biphasic solvent system of H_2O: CMPE at 170 °C within 40 min [36]. The activity of the Naflon NR-50 pellets was relatively constant for three consecutive cycles. However, the furfural yield decreases after the fourth cycle. This was attributed to the gradual deactivation of the pellets by humin deposition. Interestingly, Mittal et al. reported the possibility of simultaneously dehydrating glucose and xylose from corn stover hydrolysate to obtain a relatively high product yield using a combined Amberlyst-15 and Purolite in a one-pot reactor [37]. The reusability of the catalysts was examined five consecutive times by adding fresh solvent and substrates after each run without implementing any catalytic reactivation or washing step in between each run. While the use of ion exchange resins such as amberlyst-15, amberlyst-70, Nafion, etc as dehydrating catalysts for furfural synthesis seems admirable, the major drawbacks are the low thermochemical stability and reusability at elevated temperatures. According to the producer's datasheets, Nafion and Amberlyst-15 have a maximum operating temperature of 240 and 120 °C in aqueous system, respectively. Not to mention that these materials may shrink or swell when exposed to harsh reaction conditions.

2.1.3. Metal oxides/mixed metal

Unlike most traditional ion exchange resins, metal oxides/mixed metal solid acid catalysts generally exhibit high thermal stability, and resistance to fouling and leaching and can be reused several times without significant loss of catalytic activity. Applying a critical sonochemistry approach, Mishra et al., were able to enhance the catalytic properties of Zn-doped CuO nanoparticles, which led to a higher furfural yield of 86 %, compared to the traditional ZnO which gave a furfural yield of 45 % at the same operating conditions (150 °C, 12 h) [38]. It is worth noting that the sonochemistry created an unorganized and perturbed unit cell with many vacancies and dislocations, which are desirable features for the catalytic activities of metal oxide nanoparticles. In an on-pot reactor, Bhaumik and Dhepe obtained a furfural

yield of 71 % directly from xylan using a sol–gel synthesized silica-supported tungsten oxide with a high Lewis acidity [39]. Additionally, the synthesized WO_3/SiO_2 catalyst presented exceptional reusability in a minimum of eight catalytic runs after simple water washing. Its exceptional catalytic activity was attributed to the silicotungestic-type acid species anchored on the WO_3/SiO_2. Under continuous flow conditions for furfural production, Moreno-Marrodan et al. synthesized a non-conventional water-tolerant solid acid monolithic catalyst based on a mixed niobium-titania skeleton build-up [40]. While no significant catalytic deactivation was observed over a 4-day usage, the catalytic efficiency was greatly influenced by the niobium content in the Titania lattice. 2 wt% niobium resulted in a furfural yield of 41 % (140 °C, 141 sec in a H_2O: GVL solvent system). Table 2 presents some selected solid catalysts employed for furfural production.

2.2. Solvent effect

The selection of an appropriate solvent with a synergetic interaction between the substrate and catalyst is essential as the performance of catalysts can be largely influenced by the nature of the solvent. This synergetic interaction can significantly alter the solubility, thermodynamics, transition states, and activation energy, making it possible (to some certain extent) to control the selectivity and reaction rate by simply changing the solvent system [46].

The high rate of humin formation and furfural degradation has been linked to the use of aqueous solvent systems as industrial processes solely rely on water as the primary solvent [43]. By reason of the acidic protons solvation of water molecules, Brønsted acid catalysts can suffer from lower activity in an aqueous media [47]. Such stabilization can be reduced by the use of aprotic solvents, which decrease the stabilization of Brønsted acidic protons relative to their protonated transition states in the system [48]. To better understand this, Hu et al., investigated the involvement of 20 different conventional solvents ranging from water, alcohols, ketones, furans, esters, hydrocarbon, and aromatics with the singular aim of understanding their interactions with the substrate (xylose), catalyst (Amberlyst-70) and product (furfural) at 160 °C within 100 min [49]. Alcohols (methanol, 1-propanol, and 1-butanol) were found to promote the formation of furfural, stabilize the reactive intermediates, and slow down the degradation rate when compared with water. Isopropanol and 2-butanol slowly convert xylose directly to levulinic esters via transfer hydrogenation from the Brønsted catalyst. Solvents with a carbonyl group (acetone, hydroxyl acetone, and cyclopentanone) or/and conjugated π bond (furan, 2,5-dimethoxy tetrahydrofuran, and tetrahydrofuran) were reported to further react with xylose and/or furfural. The furfural degradation rate was reportedly high in ethers, hydrocarbons, and aromatics due to the aprotic properties. Aprotic solvents are known to influence the reaction kinetics by changing the stabilization of the acidic proton relative to the protonated transition state [50]. Alcohols such as methanol and ethanol (supercritical) have been used to enhance the depolymerization of LCB and subdue furfural degradation reactions [51,52].

However, due to the health and environmental issues arising from the use of conventional solvents such as MIBK, toluene, etc, green solvents such as ionic liquids (ILs) and deep eutectic solvents (DEs) are becoming increasingly attractive due to their non-toxicity, recyclability, low volatility, high solubility, low vapor pressure, thermochemical stability, and tuneable physical and chemical properties which can be achieved by changing the anion and cation ratio [53]. They have also been proven to act as effective Brønsted acid catalysts in aqueous media furfural production [54–57]. Ionic liquids such as $[BMIM]HSO_4$, and [EMIM]Br are even more attractive as they can simultaneously be used as catalysts and solvents/cosolvents for the production of furfural [18,58–60].

In search of an environmentally friendly and non-toxic solvent for

Table 2
Furfural production from selected solid catalyst.

Catalyst	Substrate	Solvent system	Temp. (°C)	Time	Yield (%)	Catalyst reuse	Ref
Dealuminated H-Y	Xylose	H_2O:butanol	180	30 min	77.5	66.1 %, 5 cycles	[34]
H-β	Xylose	1,4-dioxane	140	40 min	93.6	–	[30]
H-β	Xylan	1,4-dioxane	140	40 min	85.9	81.3 %, 5 cycles	[31]
SAPO-34	Xylose	H_2O:GVL	200	30	40	–	[30]
SAPO-34	Switchgrass	H_2O:GVL	200	30	31	26 %, 3 cycles	[30]
Al-Beta	Corncob	H_2O:GVL	175	100 min	47.6	35 %, 4 cycles	[40]
Fe-Beta	Corn cob	H_2O:GVL	175	100 min	40.1	–	[41]
Cr-Beta	Corn cob	H_2O: GVL	175	100 min	36.4	–	[41]
H-ZSM-5	corn cob	GVL	190	60 min	71.68	–	[41]
H-β-SO3-H	Xylose	IPA	150	7 h	76.8	51.8 %, 3 cycles	[32]
Amberlyst-70	Xylose	H_2O:CO_2	150	16 h	42.1	–	[35]
Amberlyst-15	Straw holo cellulose	H_2O: GVL	180	3 h	62	–	[42]
Nafion NR50	Xylose	H_2O: CPME	170	40 min	80	68 %, 4 cycles	[36]
Amberlyst-70	Xylose	H_2O: toluene	175	50 min	65	–	[43]
Purolite and Amberlyst-15	Corn stover hydrolysate	H_2O: dioxane	195	5 min	90	81 %, 5 cycles	[37]
Zn doped CuO nanoparticle	Xylose	H_2O	150	12 h	86	–	[38]
WO3/SiO2	Xylan	H_2O:Toluene	170	10 h	71	71 %, 8 cycles	[39]
Nb-TiO-MNL2	Xylose	H_2O:GVL	140	141 s	42	41 %, 4 days	[40]
SO_4^{2-}/Sn-DM	Corn stover	H_2O: DMSO/toluene	190	3 h	77.82	–	[44]
SO_4^{2-}/Sn-DM	Xylose	H_2O:DMSO/toluene	170	3 h	82.79	82 %, 5 cycles	[44]
SC-CaCt-700	Corn stover	GVL	200	100 min	95	61 %, 5 cycles	[44]
Porous polytriphenylamine-SO_3H	Xylose	GVL	175	45 min	73.9	70 %, 4 cycles	[45]

furfural production, Canada-Barcala et al. screened 30 natural solvents using the COSMO-RS (conductor-like screening model for real solvents) for the selection of solvents with higher affinity for furfural [61]. Amongst the selected solvents, thymol and eugenol showed extractive yields of 95 and 91 %, which was significantly higher than those of the conventional solvents MIBK (85 %) and toluene (81 %). Carvalho et al., reported the possibility of directly hydrolyzing and dehydrating Wheat straw into furfural in a one-pot reactor without additional catalystwhile using [BMIM]H_2SO_4 [62]. Although DEs and ILs show important advantages in terms of sustainability and environmental impacts, however, the cost of these solvents and the development of an effective recovery and recyclable system remains a major setback for their industrial-scale application [63]. For instance, Sen et al. cited that a minimum of 98 % recovery of [EMIM]Cl is required for economic profitability [64]. Additionally, some ILs have been reported to be highly viscous, which may encourage mass transport limitations and further hinder the separation processes [56].

Biphasic solvent systems can provide alternative routes that leverage on the differences in the hydrophobicity of the catalyst, substrate(s), and product(s), leading to a higher furfural selectivity than the conventional single-phase system. In this case, the catalyst and substrate remain in the aqueous phase where the reaction occurs while the product (furfural) is selectively extracted into the organic phase where it can be preserved from further degradation (Fig. 3). Biphasic solvent systems have gained significant attention since they can potentially prevent further furfural degradation and enhance the ease of product separation and solvent recovery. Mittal et al. showed that a furfural yield of up to 80 % can be selectively extracted using MIBK as an extractive phase in a biphasic solvent system of H_2O: MIBK at 170 °C within 20 min from corn Stover hydrolysate [24]. More recently, Liu et al. reported an increase in furfural yield from 52.5 % to 68.8 % when the aqueous solvent system was changed to a biphasic H_2O/toluene (1:1) system [65]. Table 3 presents a summary of some selected solvent systems used for furfural production.

Ideally, a biphasic solvent system would be perfectly immiscible (a distinct partition between the organic and aqueous phase), possesses a high affinity to extract furfural into the organic phase selectively, does not form an azeotrope with water, and has a wide range in boiling points to ease separation via distillation. A rule of thumb for distillation suggests a 25 – 30 °C difference in the boiling point between components for practical separation with minimal energy requirement [66].

In general, the choice of a solvent system is crucial as it contributes to the overall sustainability and economic viability of the process. While the choice of a solvent system has multiple technical and economical trade-offs (high product yield, product/catalyst separation, reduction in processing steps, reduction in humin formation, cost of solvent system, etc), environmental, health, and safety considerations should be prioritized from a life cycle impact perspective. For example, benzene, formaldehyde, dichloromethane, and trichloroethylene have been classified as toxic (carcinogenic) according to the International Agency for Research on Cancer [84]. In light of the design and operation of safer processes, the Innovative Medicines Initiative (IMI)-CHEM21 developed a solvent guide that presents explicit Safety, Health, and Environment (SH&E) criteria [85]. The health scoring reflects the occupational hazard, the safety scoring system was based on the flammability of the solvents and the environmental scoring was solely linked to ozone layer depletion, acute ecotoxicity, bio-accumulation, volatility, and recyclability. These criteria give an overall preliminary ranking of any solvent from a scale of 1 to 10, 10 indicating the highest possible hazard in each category. Additionally, a color code was introduced in the scoring: 1–3, 4–6, and 7–10 for green, yellow, and red respectively. This enables a simplified solvent greenness evaluation. A combination of these scores provides a simplified default ranking in three categories:

- Recommended: these solvents are to be screened before use to ensure chemical compatibility in the specific process conditions,
- Problematic: suitable for use in the lab while pilot or commercial scale application will necessitate specific precautions,
- Hazardous: substitution for these solvents must be a priority as the limitations on scale-up are very high.

Based on these criteria, Table 4 presents a simplified comparison of different potential solvent systems for furfural production based on their miscibility with furfural, formation of azeotrope with water and boiling points while considering their safety, health and environmental score based on the CHM21 ranking. Some bio-based solvents are, however,

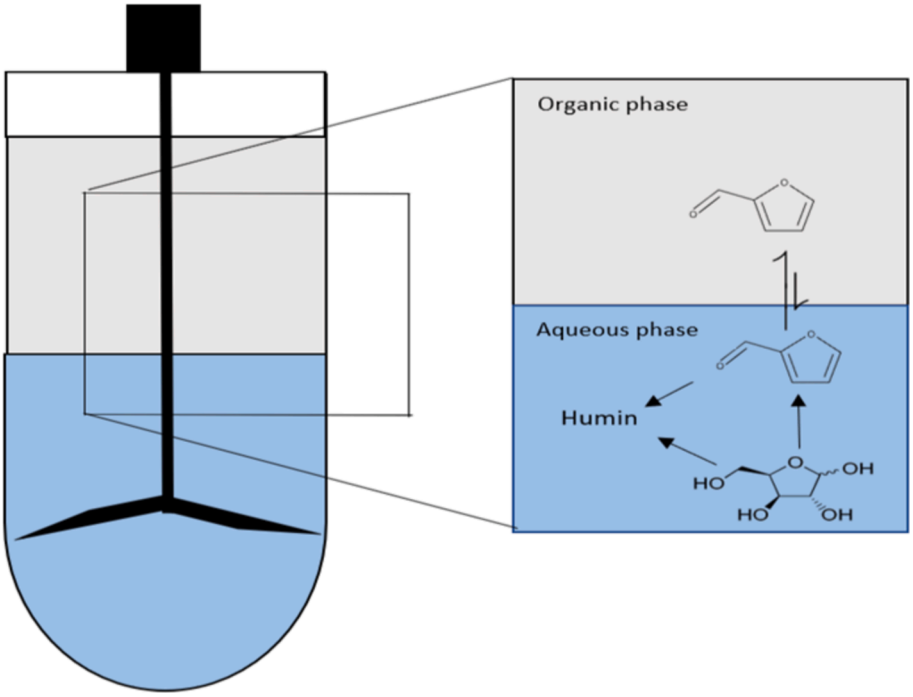

Fig. 3. Biphasic extraction of furfrual.

Table 3
Comparison of furfural production in different solvent systems (Aqueous organic, ILs, Des, and biphasic).

Solvent system	solvent	Substrate	catalyst	Temperature (°C)	Reaction time (min)	Furfural yield (%)	Reference
Aqueous	H_2O (S:L = 1:10, w/w)	Giant Miscanthus (500 mg)	H_2SO_4 (0.3 wt%)	180	30	64.39	[67]
	H_2O (60 mL)	Corncob (6 g)	SO_4^{2-}/SiO_2-Al_2O_3/La^{3+} (0.1 g)	150	150	21	[68]
	H_2O	Oil palm empty fruit bunches (20 wt%)	H_2SO_4 (1.025 % v/v)	198	11	29.6	[69]
	H_2O	Xylose (1 g/L)	$AlCl_3$ (8 mM) HCOOH (8 mM)	180	15	92.2	[70]
	H_2O (S:L = 1.17, w/w)	Corncob (100 g)	H_2SO_4 (4 w/w %), CH_3COOH (3 v/v%), $FeCl_3$ (5 g)	180	–-	68.04	[71]
Organic	95 wt% Methanol (45.6 g)	Wheat Straw (6 g)	H_2SO_4 (40 mM)	175	120	40.6	[51]
	Ethanol (S:C = 1:2, w/w)	Oil Palm Fronds (0.6 g)	HCOOH	280	20	35.8	[52]
	Gamma undecalactone (2 mL)	Corn cob (25 mg)	SPTPA (6 mg)	175	45	53	[45]
	Gamma Butyrolactone (7 mL)	Corn Storver (50 mg)	SC-CaC_t-700 (150 mg)	200	100	89	[72]
	GVL (15 mL)	Corncob (0.4 g)	PTSA-POM (0.2 g)	190	100	83.5	[73]
Ionic liquids	[EMIM]Br (1000 mg)	Xylose (200 mg)	$SnCl_4$ (C:B = 1:10 w/w)	130	60	71.1	[74]
	[BMIM]Cl (2 g)	Xylose (38 mg)	0.25 mmol $AlCl_3$ (10 μL H_2O)	170	0.6	84.8	[75]
	[BMIM]HSO_4 (S:L = 1:10, w/w)	Eucalyptus Wood (8 kg)	[BMIM]HSO_4	160	240	59.1	[59]
	[BMIM]HSO_4 (4 g)	Wheat Straw (S:B = 1:10)	[BMIM]HSO_4	161	104.5	32.2	[18]
Deep eutectic	ChCl-oxalic acid (2 g)	Xylan (38 mg)	2 g ChCl, 0.25 mmol oxalic acid, 0.25 mmol $AlCl_3{\cdot}6H_2O$	100	70	38.4	[75]
	ChCl-oxalic acid	Xylan	ChCl-oxalic acid, $AlCl_3{\cdot}6H_2O$	100	50	39.8	[75]
	ChCl-oxalic acid (88 mmol)	Oil Palm fronds (0.8 g)	ChCl-oxalic acid (88 mmol)	100	135	26.34	[76]
	ChCl-oxalic acid (5 mL)	Macuaba shell (0.1 g)	ChCl-oxalic acid (5 mL), TiO_2 (20 mg)	140	30	12	[77]
	ChCl (5.5 g), Fa (14.5 g), $SnCl_4$ (3.12 g)	Herbal residues (S:B = 20:1 w/w)	ChCl (5.5 g), Fa (14.5 g), $SnCl_4$ (3.12 g)	140	30	49.6	[78]
Biphasic system	H_2O:MIBK (2:1, v/v)	Corn stover hydrolysate (8 wt%)	H_2SO_4 (0.05 M)	170	20	80.1	[24]
	H_2O:Toluene (2:1, v/v)	Corn stover hydrolysate (8 wt%)	H_2SO_4 (0.05 M)	170	20	76.3	[40]
	H_2O:Cyclohexanol (2:1, v/v)	Corn stover hydrolysate (8 wt%)	H_2SO_4 (0.05 M)	170	20	73.8	[24]
	H_2O:CPME (1:3, v/v)	Xylose (0.75 mL, 186 mmol/L)	Starbon®450-SO_3H (25 mg)	175	1080	70	[79]
	H_2O:Toluene (2:8, w/w)	Corncob (0.5 g)	H_2SO_4 (0.1 g), $ZnSO_4$ (0.2 g)	150	360	60	[60]
	[BMIM]Cl:toluene (1:4.4, w/w)	Xylose (10 g)	[BMIM]Cl (100 g)	40	240	73.8	[65]
	H_2O:Toluene (1:1, v/v)	Xylose (100 mg)	P-Zr-SBA-15 (30 mg)	180	60	80.3	[54]
	H_2O:GVL (1:19, v/v)	Xylose (30 mg/mL)	SO_3H functionalized IL (0.1 M)	140	180	78.12	[55]
	H_2O:Toluene (3:3, v/v)	Rice husk (100 mg)	IMMHSO_4-IL (20 mg)	180	90	74.6	[80]
	H_2O:DC (1:1, v/v)	Bagasse (0.2 g)	Sn-MMT/SO_4^{2-} (0.1 g)	170	2.4 h	88.1	[66]
	H_2O:ChCl:GA (6:3:1, v/v/v)	Xylose (S:L = 0.05)	–-	160	10	62	[81]
	H_2O:Acetone (3:7, v/v)	Bagasse (7.4 wt%)	H_3PO_4 (30.5 wt%)	150	5	45.8	[82]
	H_2O:Toluene (2:8, w/w)	Pine (0.5 g)	H_2SO_4 (0.1 g), $ZnSO_4$ (0.2 g)	160	360	64.4	[82]
	H_2O:Toluene (2:8, w/w)	Birch (0.5)	H_2SO_4 (0.1 g), $ZnSO_4$ (0.2 g)	160	360	59.4	[82]
	H_2O:GVL (1:9 w/w)	Switchgrass (2 wt%)	SAPO-34 (0.048 g)	190	480	30	[30]
	H_2O:THF (1:4, v/v)	Pubescens (0.5 g)	NaCl (5 wt%)	200	120	76.9	[83]

ranked problematic by default. This was primarily due to their high boiling points, which may subsequently reflect difficulties during product separation and solvent recovery. Additionally, most bio-based solvents have yet to be considered by the "Registration, Evaluation, Authorisation and Restriction of Chemicals (REACh)" and thus score a default value of 5 in the Health and Environment criteria.

3. Overview kinetic models of furfural production

While the reaction pathway of pentose dehydration into furfural has not been generally agreed on, it has been hypothesized that its synthesis follows a pseudo-homogenous first-order irreversible reaction pathway. Different approaches have been used for the development of models describing the rate of pentose decomposition and/or furfural degradation, each with its merits and limitations.

One of the simplest models proposed for the reaction network assumes a direct dehydration of xylose to furfural without any intermediate [86]. Decomposition products such as condensation and resinification are also possible within this reaction pathway [87] as illustrated by Fig. 4. Jing and Lü studied the non-catalytic decomposition of D-xylose into furfural under high-temperature liquid water (HTLW) and also verified that the reaction pathway was plausible at a wide temperature range (180 – 220 °C) [88]. While the main products obtained were furfural and formic acid, Jing and Lü observed a further degradation of the xylose and furfural into insoluble dark-brown substances (humin) under the HTLW conditions. Jing and Lü found the model to be in good agreement with their experimental data, and the activation energy of xylose dehydration and furfural decomposition were 123.27 and 58.84 kJ mol^{-1}, respectively. Ershova et al. applied this model during their studies on the roles of various chlorides in the dehydration of xylose. With the exception of dibasic salts, the kinetic model fitting was reported to be a good agreement with their experimental data.

One of the most widely employed pseudo-homogenous models for furfural production was proposed by Dunlop in 1948 [89]. According to his theory, xylose is able to generate intermediates during its direct

Table 4
Solvent properties, health, safety, and environmental impact scores based on the CHEM21 default ranking [85].

Solvent	Boiling point (°C)	Flash point (°C)	Safety score	Health score	Environment score	CHEM21 ranking by default
Gamma-Valerolactone	207	23	1	5	7	Problematic
i-Butanol	107	28	3	4	3	Recommended
Methanol	65	11	4	7	5	Recommended
Ethanol	78	13	4	3	3	Recommended
i-Propanol	82	12	4	3	3	Recommended
n-Butanol	118	29	3	4	3	Recommended
Ethyl Acetate	77	−4	5	3	3	Recommended
Tetrahydrofuran	66	−14	6	7	5	Problematic
Dimethyl Sulfoxide	189	95	1	1	5	Recommended
Acetonitrile	82	2	4	3	3	Recommended
i-Butyl Acetate	115	22	4	2	3	Recommended
Methyl Tetrahydrofuran	80	−11	6	5	3	Problematic
Cyclopentyl Methyl Ether	106	−1	7	2	5	Problematic
Diethyl Ether	34	−45	10	3	7	Hazardous
DME	85	−6	7	10	3	Hazardous
1,4-Dioxane	101	12	7	6	3	Problematic
Benzene	80	−11	6	10	3	Hazardous
Toluene	111	4	5	6	3	Problematic
MIBK	117	13	4	2	3	Recommended

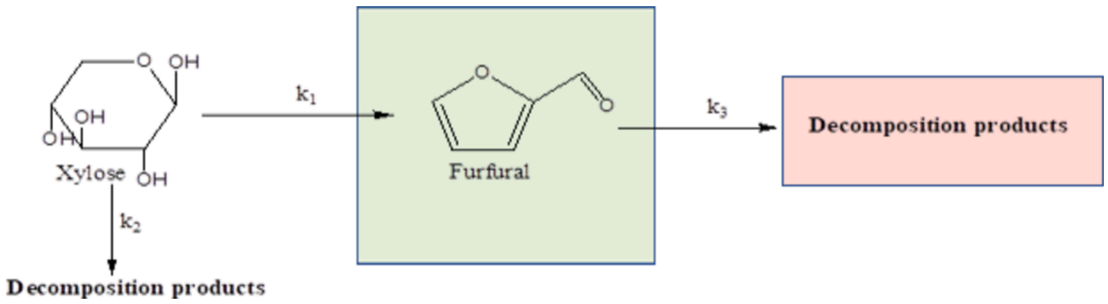

Fig. 4. Model – 1: Furfural formation and direct xylose decomposition.

dehydration. The formed intermediate products subsequently dehydrate to furfural. During this process, condensation (reaction between the intermediate products and furfural) and decomposition of furfural are bound to happen. Dunlop also added that it would be impossible to measure the concentrations of the intermediates experimentally, suggesting an instantaneous exists as depicted in Fig. 5. Chen et al., confirm the validity of Dunlop's model while studying the kinetics of xylose dehydration into furfural in acetic acid. Chen's experimental data conforms to the first-order reaction as it was found that both xylose dehydration and furfural decomposition rates were dependent only on the initial xylose concentration. Chen also noted that the furfural degradation into decomposition products has little effect on the overall furfural yield, while the condensation reactions (reaction between the formed furfural and the intermediates) are the fundamental reason for low furfural yield [90]. This statement was backed up by the fact that the rate constant of xylose dehydration was way higher than that of furfural degradation but was almost near to the condensation rate constant. Investigating the acid dehydration of xylose over a wide range of sulphuric acid concentrations, Krzelj et al., suggest an additional intermediate product based on their experimental observations [91]. While they affirm the fact that these intermediates could not be measured experimentally as previously proposed by Dunlop, a lumped intermediate was forged with the assumption that one of the intermediate rate of dehydration happens way faster than the other (i.e., $k_1 \gg k_2$). Within the limits of experimental constraints, Krzelj strongly supports Dunlop's claim that xylose does not react directly with furfural and xylose degradation intermediates are an important pathway toward furfural degradation and selectivity loss. (Fig. 6).

This was not the case for Marcotullio and De Jong, as they strongly affirm that xylose undergoes further side degradation reactions that lead to the formation of humins [92]. This additional reaction step was included in the Dunlop's model. While the modified model showed good

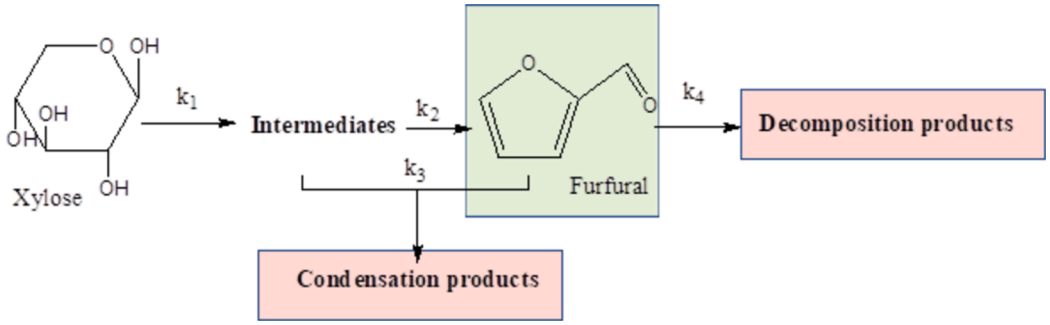

Fig. 5. Model – 2: Furfural formation with side reaction between intermediates and furfural.

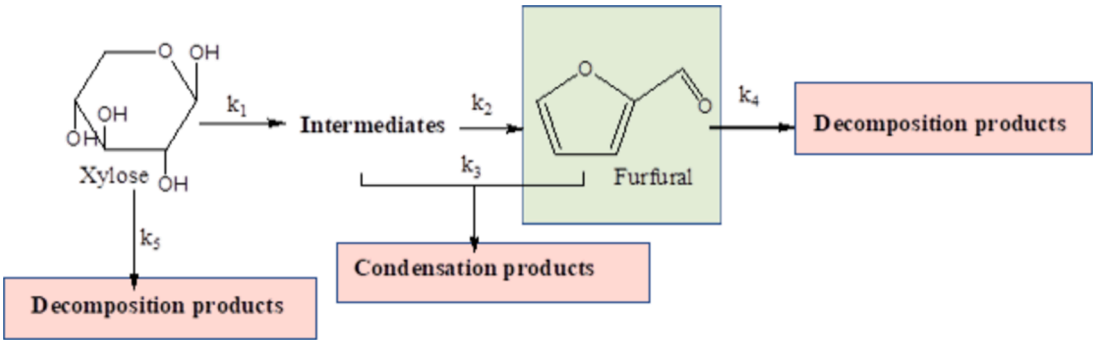

Fig. 6. Model – 3: Furfural formation with direct xylose decomposition and side reaction with intermediates.

agreement with the experimental data, the kinetic parameters showed a similar dependence on the acid concentration as initially proposed.

The high activation barrier (> 100 kJ.mol^{-1}) necessitating operating at a high-temperature regime (>150 °C) and longer reaction time are the major setbacks in the direct dehydration of xylose to furfural catalyzed by a Brønsted acid site (Model-1, Model-2, and Model-3). Choudhary et al., recently showed that the mechanistic pathway of xylose dehydration can be altered leading to a corresponding increase in furfural yield when catalysts having both Lewis and Brønsted acid sites are applied [93]. The Lewis acid sites isomerize xylose into its corresponding isomers (xylulose and xylose), while the Brønsted acid sites subsequently dehydrate both the isomers and xylose into furfural Fig. 7. Catalysts equipped with Lewis and Brønsted acids can lower the activation barrier by altering the reaction pathway. Choudhary et al. observed this change during a systematic examination of the role of $CrCl_3$ and HCl on the molecular structure of pentose during its dehydration to furfural in a single aqueous phase media. They concluded that the contribution of each pathway (direct dehydration and isomerization) largely depends on the operating temperature and the Lewis and Brønsted acid concentration ratio. In an attempt to fully understand the role of the reaction pathway on the kinetics of xylose dehydration, Ershova et al. studied the dehydration of xylulose to furfural and the relevance of xylulose as an intermediate product during xylose dehydration to furfural [94]. It was shown that the rate of furfural formation was much lower from xylulose dehydration than from xylose dehydration. While their experimental result ruled out xylulose as a key intermediate during xylose dehydration, the developed model helped establish its role along a parallel reaction pathway.

Due to the heterogeneous nature and complexity of hemicellulose structure, most studies on furfural kinetics consider xylose a good representative of depolymerized hemicellulose. Unlike cellulose, which solely consists of repeating glucose units connected by β-1,4-glucosidic linkage, hemicellulose is structurally diverse. Depending on its source, it consists primarily of xylan and other polysaccharides such as arabinoxylan, arabinan, and galacto-glucomannan (Fig. 8). Hence, developing a realistic and well-detailed kinetic model of furfural production directly from hemicellulose is challenging. Despite these challenges, a few studies have attempted to model furfural kinetics directly from hemicellulose. Nabarlatz et al. developed a kinetic model for the autohydrolysis of xylan in lignocellulosic biomass that describes the yields of the different reaction products and explains the changes in the chemical composition of the *xylo*-oligomers due to reaction temperature and time [95]. Their model assumed xylan, the major constituent of hemicellulose consists of a xylose unit backbone connected to side groups such as arabinose and acetyl substituents.

Furthermore, the model identifies two xylan fractions with different reactivities towards hydrolysis (fast and slow hydrolysis). The monosaccharides from the hydrolysis step, namely xylose and arabinose, degrade to furfural and degradation products. The model was validated over experimental data obtained from the autohydrolysis of corncob in a batch reactor at a temperature range of 150 – 190 °C.

A summary of the kinetic information and pathways for selected studies of furfural production from LCB and pentose are detailed in Table5.

Concerning catalyst design, kinetic models are of prime importance because they give fundamental information about the reaction mechanisms and help pinpoint the rate-limiting or rate-controlling steps. Understanding such models, in turn, enables the design of catalysts that can either promote desired reactions or suppress undesired side reactions like the condensation between the intermediates and furfural, which significantly affects the yield of furfural. By employing such kinetic insights, researchers will gain better control over reaction variables and, with that, move closer to enhancing the chances of more effective and greener catalyst development for biomass conversion processes.

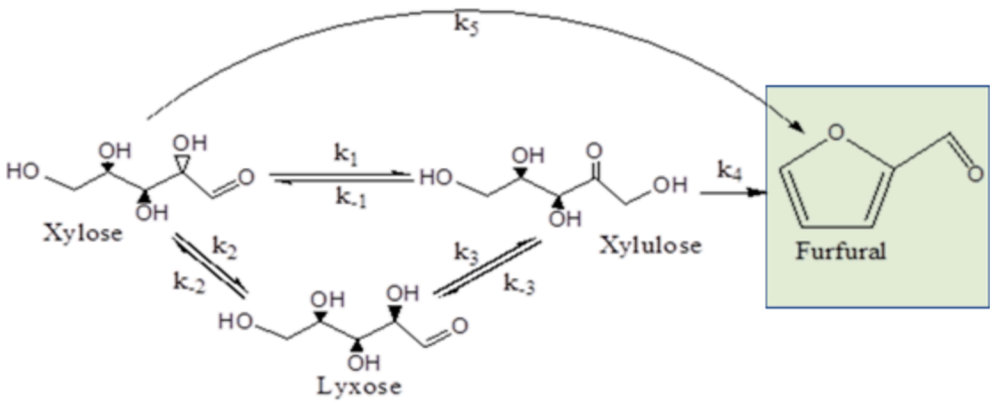

Fig. 7. Model – 4: Furfural formation via isomerization and dehydration.

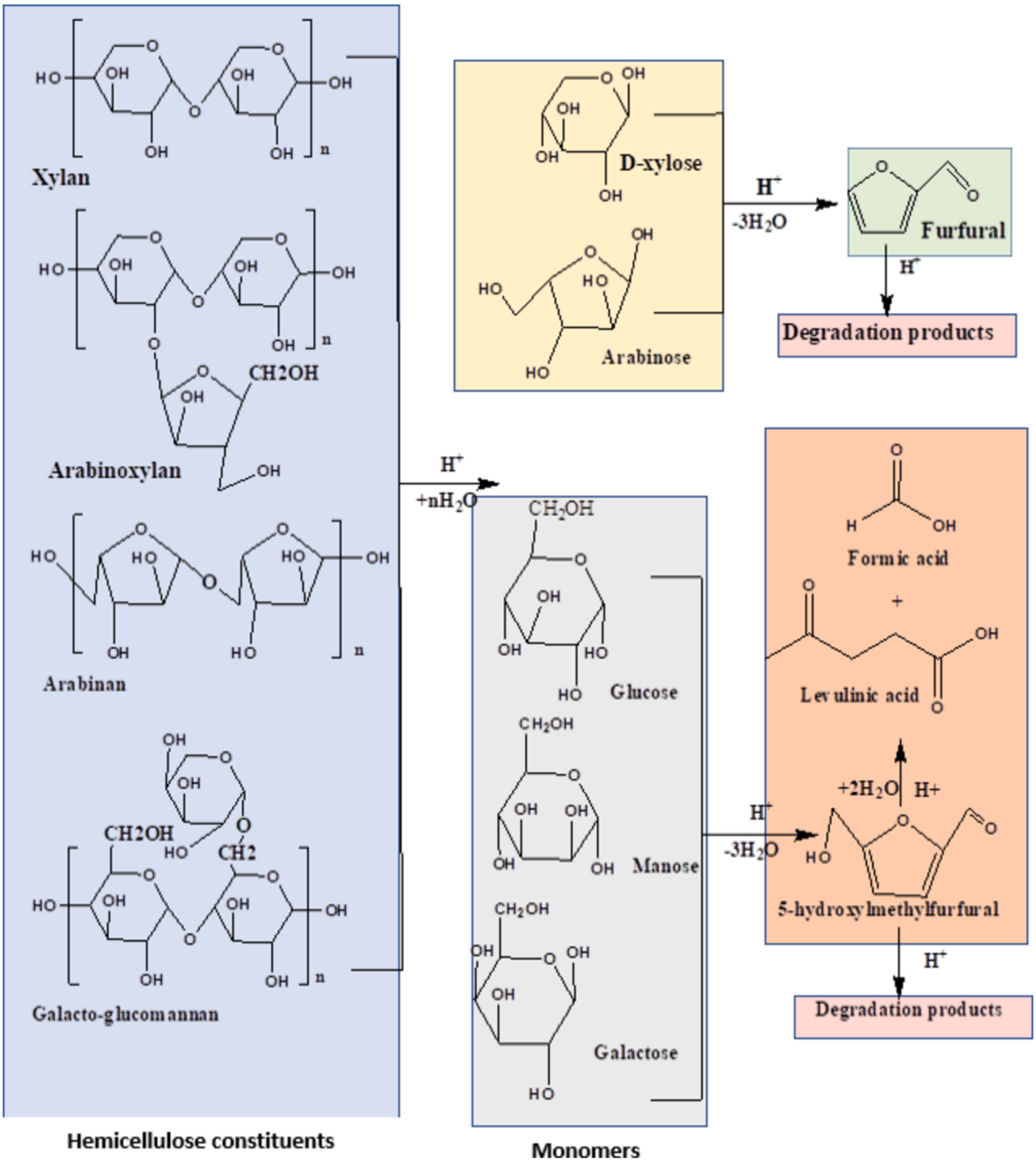

Fig. 8. Acid-catalyzed hydrolysis network of hemicellulose in lignocellulosic biomass.

4. Process intesification

Beyond the design of new heterogeneous catalysts and the selection of green solvents, several studies have shown that low furfural yield due to a high rate of humin formation can be resolved via process intensification strategies. Conventionally, the furfural production process consists of four major steps on a commercial scale: mineral acid hydrolysis of hemicellulose-rich lignocellulosic biomass into pentose, dehydration of pentose into furfural, recovery of furfural from the reaction medium and purification. The Quaker oats batch process was the first industrial process for producing furfural. This process was developed in 1922. The Quaker's process was based on the digestion of Oat hulls by sulphuric acid in a batch reactor. The generated furfural was stripped off the reaction medium by a continuous injection of steam at 153 °C within 5 h. The stripped furfural, alongside other by-products, are condensed and transported to an azeotropic distillation column to separate furfural from water and other by-products. While the continuously injected steam minimizes furfural degradation due to resinification and condensation reactions, the process was characterized by low furfural yield (<50 %), high amount of acidic residual, long reaction time, and high energy demand [96]. The high steam-to-furfural ratio leads to a diluted furfural remains a major industrial limitation. Additionally, the heterogeneous azeotrope formed between furfural and water requires substantial energy to concentrate furfural via distillation. In an attempt to overcome these limitations, the Quaker's process was modified from a batch to a continuous process. Superheated steam was used to strip off the generated furfural from the reaction medium at 184 °C within an hour. Despite the modification, there was no significant improvement in the process. Other interesting industrial processes such as the Chinese batch process, the Westpro-modified Huaxia

Table 5
Selected kinetic studies of furfural synthesis from lignocellulosic biomass and pentose.

Reaction pathway	Developed rate expression	Operating condition, reactor, catalyst, and solvent	Rate constant (min^{-1})	Activation energy (kJ mol^{-1})	Ref.
Xylose $\rightarrow^{k_1}$ Xylulose Xylulose $\rightarrow^{k_2}$ Furfural Xylose $\rightarrow^{k_3}$ Furfural Furfural $\rightarrow^{k_4}$ DP_3 Xylulose $\rightarrow^{k_5}$ DP_2 Xylose $\rightarrow^{k_6}$ DP_1	$\frac{d[X]}{dt} = -(k_1+k_5+k_4)[X]$ $\frac{d[I]}{dt} = k_1[X]-(k_4+k_5)[XI]$ $\frac{d[F]}{dt} = k_4[XI] + k_5[X] - k_4[F]$	$Xylose_{(0)}$ = 7 mmol/L Reactor type = Glass vial Temperature = 180 – 220 °C Furfural yield max = 65 %, 220 °C Time = 3 min Agitation = 600 rpm Catalyst = 0.1 mol/L H_2SO_4 Solvent = H_2O	k_1 = 0.056 k_2 = 16.151 k_3 = 2.499 k_4 = 0.0315 k_5 = 11.214 k_6 = 1.235	E_1 = 67.4 E_2 = 132.9 E_3 = 166.2 E_4 = 72 E_5 = 134.5 E_6 = 162.9	[94]
Xylose $\rightarrow^{k_1}$ $Furfural_{(aqu)}$ Xylose $\rightarrow^{k_2}$ Humin $Furfural_{(aqu)} \leftrightarrow$ $Furfural_{(org)}$	$\frac{d[X]}{dt} = -(k_1+k_2)[X]\left\lvert\frac{d[X]}{dt}\right\rvert t < t_1 = -k_1[X]$ $\left\lvert\frac{d[Humins]}{dt}\right\rvert t \geq t_1 = k_2[X]\frac{[Humins]}{[Xylose]_0} = 1-\exp(-k_1 t)$	$Xylose_{(0)}$ = 1.2 mol/L Reactor type = Batch Autoclave Temperature = 120 – 160 °C Catalyst = 10 mol % $FeSO_4$ Solvent = H_2O: 2-MTHF Furfural max yield = 44 %,140 °C	k_1 = 0.0035 k_2 = 33.33	E_1 = 151 E_2 = 139	[98]
Xylose $\rightarrow^{k_1}$ Furfural Furfural $\rightarrow^{k_2}$ DP Xylose + Furfural $\rightarrow^{k_3}$ CP	$\frac{d[X]}{dt} = -k_1[X]$ $\frac{d[F]}{dt} = -k_2[F]$ $\frac{d[DP]}{dt} = k_3[X][F]$	$Xylose_{(0)}$ = 80 g/L Reactor type = Autoclave Temperature = 170 – 210 °C Agitation = 400 rpm Catalyst = Acetic acid (0.5mo/L) Solvent = H_2O Furfural max yield = 200 °C	k_1 = 0.0374 k_2 = 0.0009 k_3 = 0.0772	E_1 = 108.6 E_2 = 63.413 E_3 = 104.99	[90]
Xylose $\rightarrow^{k_1}$ Furfural Furfural $\rightarrow^{k_2}$ DP	$\frac{d[X]}{dt} = -k_1[X]$ $\frac{d[F]}{dt} = k_1[X]-k_2[F]$	$Xylose_{(0)}$ = 3 g Reactor type = Autoclave Temperature = 170 – 120 °C Pressure = 0 bar Catalyst = Glu-TsOH-Zr (0.5 g) Solvent = H_2O (50 ml) Furfural max yield = 12.6 %, 190 °C	k_1 = 0.0162 k_2 = 0.0024	E_1 = 222.18 E_2 = 104.56	[99]
Xylose $\rightarrow^{k_1}$ Furfural Xylose $\rightarrow^{k_2}$ DP Furfural $\rightarrow^{k_3}$ DP	$\frac{d[X]}{dt} = -k_1[X]-k_2[X]$ $\frac{d[F]}{dt} = k_1[X]-k_3[F]$	$Xylose_{(0)}$ = 0.05 mol/L Reactor type = Autoclave Temperature = 160 – 200 °C Pressure = Autogenous Cat. = 0.5 mol/L HCl + 0.5 m/LNaCl Solvent = H_2O Furfural max yield = 200 °C	k_1 = 0.0082 k_3 = 0.0066	E_1 = 133.3 E_2 = 125.8 E_3 = 102.1	[100]
Xylan $\rightarrow^{k_1}$ Furfural Furfural $\rightarrow^{k_2}$ DP	$\frac{d[X]}{dt} = -k_1[X]$ $\frac{d[F]}{dt} = k_1[X]-k_2[F]$ $\frac{d[DP]}{dt} = k_2[F]$	Corn cob $_{(0)}$ = 490 g/L Catalyst = 35 g/L H-ZSM-5 Reactor type = Autoclave Temperature = 170 – 210 °C Furfural yield max = 71.68 %, 190 °C Time = 60 min Solvent = H_2O: GVL	k_1 = 0.0341 k_2 = 0.0061	E_1 = 67.67 E_2 = 55.2	[101]
Hemicellulose $\rightarrow^{k_1}$ furfural Furfural $\rightarrow^{k_2}$ *DP*	$\frac{d[H]}{dt} = -k_1[H]$ $\frac{d[F]}{dt} = k_1[H]-k_2[F]$ $\frac{d[DP]}{dt} = k_2[F]$	Eucalyptus sawdust = 0.4 g Catalyst = 30 g/L H-SAPO-34 Reactor type = Autoclave Solvent = H_2O:GVL Temperature = 190–210 Time = 120 min Furfural yield max = 99.28 %, 210 °C	k_1 = 0.047 k_2 = 0.0004	E_1 = 120.41	[102]

(*continued on next page*)

Table 5 (*continued*)

Reaction pathway	Developed rate expression	Operating condition, reactor, catalyst, and solvent	Rate constant (min^{-1})	Activation energy (kJ mol^{-1})	Ref.
Xylose $\rightarrow^{k_1}$ Furfural Xylose $\rightarrow^{k_2}$ DP_1 Furfural $\rightarrow^{k_3}$ DP_2 Xylose $\rightarrow^{k_4}$ Intermediate Intermediate $\rightarrow^{k_5}$ Furfural Intermediate $\rightarrow^{k_6}$ DP_3 Furfural $\rightarrow^{k_7}$ DP_4	$\frac{d[X]}{dt} = -(k_1+k_2+k_4)[X]\frac{d[I]}{dt} = k_4[X]-(k_5+k_6)[I]\frac{d[F]}{dt} = k_1[X]+k_5[I]-(k_3+k_6)[F]$	$Xylose_{(0)}$ = 186 mmol/L Catalyst = 50 mg Sulfated zirconia Temperature = 170 – 210 °C Reactor type = microwave batch Solvent = H_2O Time = 2 min Furfural yield max = 41 %, 210 °C	k_1 = 0.028 k_2 = 0.014 k_3 = 0.004 k_4 = 2.02 k_5 = 2.41 k_6 = 3.71 k_7 = 0.008	E_1 = 121 E_2 = 103 E_3 = 53.7 E_4 = 122 E_5 = 161 E_6 = 164 E_7 = 73	[103]
Xylose $\rightarrow^{k_1}$ Furfural Xylose $\rightarrow^{k_2}$ Intermediate Intermediate $\rightarrow^{k_3}$ Xylose Intermediate $\rightarrow^{k_4}$ Furfural Xylose $\rightarrow^{k_5}$ DP Furfural $\rightarrow^{k_6}$ DP Intermediate $\rightarrow^{k_7}$ DP	$\frac{d[X]}{dt} = -(k_1+k_2+k_5)[X]+k_3[I]\frac{d[I]}{dt} = k_2[X]-(k_3+k_4+k_7)[I]\frac{d[F]}{dt} = k_1[X]+k_4[I]-k_6[F]\frac{d[DP]}{dt} = k_5[X]+k_6[F]+k_7[I]$	Xylose:catalyst = 4:1 Catalyst = H-β (Si/Al = 19) Temperature = 130 – 170 °C Solvent = 2-propanol	k_1 = 0.0196 k_2 = 0.269 k_3 = 0.1802 k_4 = 0.0273 k_5 = 0.0157 k_6 = 0.0013	E_1 = 57 E_2 = 83.6 E_3 = 135.9 E_4 = 447.8 E_5 = 83.7 E_6 = 15.9	[104]
Xylose $\rightarrow^{k_1}$ Furfural Xylose $\rightarrow^{k_2}$ DP	$\frac{d[X]}{dt} = k_1[X]\frac{dDP}{dt} = k_2[DP]$	Xylose = 0.1 g Catalyst = 0.05 g $FeCl_X$-D008 Time = 120 min Solvent = GVL Temperature = 100 – 160 °C Furfural yield max = 96.3 %, 130 °C	k1 = 0.0024 k2 = 0.0021	E_1 = 98.87 E_2 = 80.13	[105]
Hemicellulose $\rightarrow^{k_1}$ xylose Hemicellulose $\rightarrow^{k_2}$ xylan Xylan $\rightarrow^{k_3}$ xylose Xylose $\rightarrow^{k_4}$ Furfural Xylose $\rightarrow^{k_5}$ DP Furfural $\rightarrow^{k_5}$ DP	$\frac{d[H]}{dt} = -(k_1+k_2)[H]\frac{[Xn]}{t} = k_2[H]-k_3[Xn]\frac{d[X]}{t} = k_1[H]+k_3[Xn]-(k_4+k_5)$ $[X]\frac{d[X]}{t} = k_1[H]+k_3[Xn]-(k_4+k_5)[X]\frac{d[F]}{t} = k_4[X]-k_6[F]\frac{d[DP]}{t} = k_5[X]+k_6[F]$	Sugarcane straw (S:L) = 1: =10 w/v Time = 15 min Solvent = H_2O Temperature = 180 – 210 °C Agitiaiton = 200 rpm Hemicellulose yield max = 85 %, 195 °C	k_1 = 0.0041 k_2 = 0.0988 k_3 = 0.0662 k_4 = 0.0316 k_5 = 0.0655 k_6 = 0.0047	E_1 = 62.68 E_2 = 109.49 E_3 = 220.23 E_4 = 122.57 E_5 = 146.47 E_6 = 119.91	[106]
$Xylan_1$ $\rightarrow^{k_1}$ xylanoligomers $Xylan_2$ $\rightarrow^{k_2}$ xylanoligomers Xylanoligomers $\rightarrow^{k_3}$ xylose Xylose $\rightarrow^{k_4}$ Furfural Furfural $\rightarrow^{k_5}$ DP Xylanoligomers $\rightarrow^{k_6}$ arabinose Arabinose $\rightarrow^{k_7}$ Furfural Xylanoligomers $\rightarrow^{k_8}$ acetic acid	$Xn = Xn_1 + Xn_2\frac{d[Xn_1]}{t} = -k_1[Xn_1]\frac{d[Xn_2]}{t} = -k_2[Xn_2]\frac{d[XO]}{t} = k_1[Xn_1]+k_2[Xn_2]-(k_3([m_{XO}]-[m_X])+k_6([m_{XO}]-[m_{ar}])+k_8([m_{XO}]-[m_{ac}]))[XO]\frac{d[Xn_1]}{t} = k_3([m_{XO}]-[m_{Xn_1}])[XO]-k_4[Xn]\frac{d[Ar]}{t} = k_6([m_{XO}]-[m_{ar}])[XO]-k_7[Ar]\frac{d[Ac]}{t} = k_8([m_{XO}]-[m_{Ac}])[Ac]\frac{d[F]}{t} = k_4[X]+k_7[Ac]-k_5[F]\frac{d[DP]}{t} = k_5[F]$	Corncob = 2.5 g Time = 330 min Solvent = H_2O Temperature = 150 – 190 °C Hemicellulose yield max = 85 %, 179 °C	k_1 = 31.52[a] k_2 = 61.4[a] k_3 = 27.55[a] k_4 = 29.36[a] k_5 = 32.48[a] k_6 = 25.08[a] k_7 = 29.82[a] k_8 = 14.18[a]	E_1 = 127.3 E_2 = 251.7 E_3 = 119.0 E_4 = 122.5 E_5 = 132.0 E_6 = 106.2 E_7 = 125.2 E_8 = 65.1	[87]
Xylan $\rightarrow^{k_0}$ xylose Xylose $\rightarrow^{k_1}$ Intermediate Intermediate $\rightarrow^{k_2}$ Furfural Intermediate + furfural $\rightarrow^{k_3}$ CP Furfural $\rightarrow^{k_F}$ DP	$\frac{d[Xn]}{t} = -k_0[Xn]\frac{d[X]}{t} = k_0[Xn]-k_1[X]\frac{d[I]}{t} = k_1[X]-k_2[I]-k_3[I][F]\frac{d[F]}{t} = k_2[I]-k_3[I][F]-k_F[F]$	Organosolv hemicellulose = 70 kg Time = 330 min Solvent = 150 kg (water: ethanol, 1:1) Catalyst = 0.8 wt% H_2SO_4 Temperature = 160 – 200 °C	k_0 = 0.01379 k_1 = 0.0007 k_2 = 0.00138 k_3 = 0.00011 k_4 = 0.00011	E_0 = 67.1 E_1 = 47.1 E_2 = 114 E_4 = 44.16	[107]

continuous process, the Rosenslew continuous process, and many more, have been developed. However, the limitation remains more or less the same. For example, about 35 tons of steam is required for every ton of furfural produced during the Westpro-modified Huaxia continuous process [97], and over 30 tons of steam is required to produce 1 ton of furfural during the Rosenlew continuous process [29]. Herein, we present innovative process intensification technological strategies proposed for furfural production, ranging from non-conventional reactors to hybrid reaction-separation configurations.

4.1. Intensification via reactive separation

Reactive separation such as reactive distillation, stripping, and extraction are recently emerging technologies employed to intensify bio-based feedstock processes. Applied to furfural production, these technologies can prevent furfural degradation while simultaneously and continuously stimulating its recovery. These technologies have proven to be important alternatives to the conventional reactor-separator configurations in systems where a high rate of side degradation is prominent [108].

Reactive distillation processes can provide unique advantages over the conventional reactor-separation set-up as furfural is immediately separated from the reaction zone as soon as it is generated, subsequently minimizing its degradation and by-product formation. Metkar et al. reported over 75 % furfural yield via continuous reactive distillation of pre-hydrolysate liquor (PHL) using H-mordenite (Si:Al = 10) as a solid acid catalyst in sulfolane [109]. Köchermann and Klemm showed that the side degradation of furfural can be prevented with a corresponding furfural yield of over 83 mol % (depending on the temperature and substrate) via hydrothermal reactive distillation [110].

Nitrogen has been alighted as a more economical stripping alternative to steam due to its inert nature, ease of separation, and recyclability, which may correspondently lead to a reduction in the total annual cost of the overall process. More importantly, nitrogen, compared to steam, does not dilute furfural in the vapor stream when condensed [111]. Also, the use of non-condensable gases such as CO_2 and H_2 has been proposed to be an effective alternative to the conventional steam stripping process since such fluids have the potential advantage of increasing the selectivity of the reaction while maintaining high conversion [112]. Additionally, CO_2 can enhance the acidity of aqueous media by forming carbonic acid, resulting in a faster dehydration rate [113]. Sato reported a higher furfural yield of up to 52.3 % when a continuous flow of supercritical CO_2 was used as an extractive agent compared to conventional organic solvents [35]. With a continuous supply of supercritical CO_2 (serving as a catalyst and stripping agent), about 56.6 mol% of furfural was stripped off from a two-stage reaction system [114]. The system consists of an extraction stage where wheat straw is hydrolyzed to hemicellulose using high CO_2 pressure and subsequent furfural production from pentoses dehydration in a biphasic solvent system consisting of water, tetrahydrofuran (THF) and methyl isobutyl ketone (MIBK) at elevated temperature. There was no introduction of a catalyst as the CO_2 formed carbonic acid with water at elevated temperatures. Furthermore, the addition of supercritical CO2 has been reported to alter the reaction pathway via the isomerization of xylose to xylulose with a higher furfural yield [115].

It is worth mentioning that extractive reaction, which involves the use of a solvent to continuously remove furfural from the reactive medium (usually the aqueous phase), has been employed as a technique to effectively shift the equilibrium towards furfural formation, thus reducing humin formation. This, however, was discussed in the previous section under solvent effect.

4.2. Intensification via non-conventional energies

Microwave-assisted heating is conceptually different from conventional heating, as it leads to energetic coupling at the molecular level, resulting from the selective interaction of electromagnetic radiation with matter [116]. During this process, the energy carried by the electromagnetic radiation is converted into thermal energy within the matter [117]. Under these conditions, the thermal effects observed are due to the heterogeneities of the microwave field within the matter, the inverted heat transfer, and the selective absorption of the radiation by polar compounds. These thermal effects can be harnessed to improve processes, enhance product selectivity, and even enable reactions that are not otherwise feasible under normal conditions. Compared to conventional heating, several studies on furfural production claim significant reaction rate enhancement under microwave-assisted heating [79,118,119]. An increase in furfural yield has also been reported due to the synergetic effect of ions and microwave-assisted heating [120].

Studies on thermal effects such as inhomogeneous heating affirm that microwave-assisted heating does not improve selectivity in monophasic aqueous xylose solution [121–123]. However, kinetic analysis confirms a 7–13 times higher rate constant for xylose dehydration under microwave-assisted heating than conventional heating [116].

In a recent study, Ricciardi et al. showed that combining microwave-assisted heating and reactive extraction can create a synergic effect that promotes higher furfural yield [124]. In this scenario, themicrowave radiation selectively heats the reactive phase (aqueous phase for efficient reaction) without excessively heating the extractive phase (organic phase for efficient extraction) as illustrated in Fig. 9. At these conditions, the symmetries in dielectric constants and volumes of the reactive and extractive phases are maximized, resulting in an asymmetric thermal response of the two phases. An optimal furfural yield of 80 mol% was obtained compared to 65 mol% under conventional heating biphasic conditions. The yield boost was attributed to the suppressed acid-catalyzed degradation and condensation of furfural due to its safe extraction and storage in the organic phase with lower temperature (compared to the aqueous phase), which can solely be achieved by microwave-assisted heating.

Despite the benefits associated with the use of microwave heating, special care must be paid to the reactor material, which must be microwave transparent, enhancing effective energy transfer and process efficiency. Materials such as Teflon, glass, silicon carbide, and quartz are commonly used as they allow microwaves to pass through while keeping the focus on heating the reactive. Energy losses, uneven heating, and possible reactor damage could occur if a material that absorbs microwave (such as metals) is used for the reactor design. This consideration becomes more critical during process scale-up, as it may lead to local hotspots, where the temperature distribution profile across the reactor is uneven, promoting side degradation reactions and decomposition of sensitive compounds or even structural damage to the reactor itself. This consideration becomes very important for processes like furfural production, where precise control over operating conditions is vital to maximize product yield and minimize side degradation.

On the other hand, ultrasound energy has also been considered to play a significant role in process intensification. Once a reaction medium

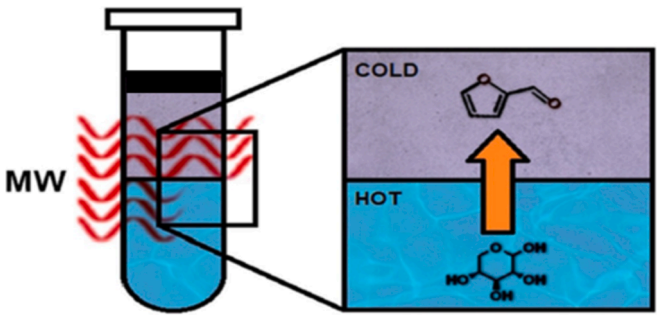

Fig. 9. Effect of an asymmetric response in the biphasic system on reactive extraction of furfural using microwave-assisted heating [124].

is sonicated, an increase in the convective and acoustic cavitations is observed which enhances mass transport and subsequently leads to higher production of radicals in the reactive system [120]. While the majority of studies have reported the synergic effects of ultrasound are related to biomass pre-treatments such as ultrasound-assisted lignification [125], ultrasound-assisted saccharification [126], etc a few focus on intensifying furfural production via ultrasound. Bizzi et al. investigated the influence of ultrasound energy on several lignocellulosic biomass (sugar cane straw, rice husk, yerba-mate waste, grass, and wood waste) conversion to furfural by acid hydrolysis and compared the obtained furfural yield with those under silent conditions [120]. The ultrasound energy was delivered to the reaction medium using a cup horn system operated at 20 kHz. SEM images before and after the experiments confirm that ultrasound energy resulted in structural modifications of the biomass, thus improving the acid hydrolysis even at room temperature (30 °C) and reducing reaction time (60 min).

4.3. Intensification via non-conventional reactor

Conventional batch reactors are often characterized by poor heat and mass transfer and limited flow pattern control, which may lead to low reactor performance when scaled-up [134]. As an alternative to conventional reactors, microreactors, vaporization reactors, membrane reactors, and catalytic bed reactors, to mention a few are regarded as efficient and key units for process enhancement and intensification. These non-conventional reactors are designed based on process parameters such as microchannel dimensions, mechanical factors, transport rate, heat flux, pressure, and temperature considerations. Compared to a conventional reactor, a higher furfural yield was reportedly obtained from a membrane reactor based on the Zn(bim)4-PMPS mixed matrix membrane [131]. The result indicates that a properly designed membrane can selectively and continuously absorb furfural as soon as it is generated from the reactive medium. Why this displays promising industrial application, the stability of membranes might be questionable under harsh reaction conditions (high temperature, acid concentration). Guo et al. demonstrated that a furfural yield of over 93 % can be obtained from a slug flow microreactor within a few minutes (4 min) [133]. A recent study demonstrates the use of a millireactor as an intensified technology for continuous furfural production. Due to the high extraction rate aided by strong inner circulation and short residence time that can be achieved by millireactor, humin formation due to side degradation reactions can be minimized [129]. Selected process intensification strategies for improved furfural production are summaried in Table 6.

5. Solvent separation and product purification

Product separation and purification are critical stages in any chemical production process as they can significantly impact the product(s) quality, applicability, and market values. To meet the ever-evolving market requirements, and regulatory standards and ultimately substitute petrochemicals, efficient separation and purification technologies must be developed for bio-based processes.

Conventional distillation remains the most widely used industrial approach for purifying furfural due to its high processing capacity and ease of application. Nonetheless, due to the heterogeneous azeotrope between furfural and water, extracting a substantial volume of water via distillation requires much energy. For example, the Westpro-modified Huaxia continuous process requires over 35 tons of steam for every ton of furfural produced [97], and over 30 tons of steam is required to produce 1 ton of furfural during the Rosenlew continuous process [29]. The high steam-to-furfural ratio is the major downside in terms of energy requirement, making the process highly energy-demanding.

In an attempt to tackle these industrial challenges, Conteras-Zarazua et al. proposed four different intensified distillation sequences for furfural purification, which include the thermal couple configuration (TCC), thermodynamic equivalent configuration (TEC), divided wall column configuration (DWCC) and heat integrated configuration (HIC)

Table 6
Selected process intensification strategies for improved furfural production.

Process intensification technology	Feedstock	Solvent and catalyst system	Process conditions	Furfural yield (%)	Reference
Reactive distillation	Xylose	Solvent = Sulfolane Catalyst = H-mordenite (10)	Feed flow rate = 0.75 mL min^{-1} Temp = 175 °C	75	[109]
	Beachwood shavings	Solvent = H_2OCatalyst = H_3PO_4	Time = 150 minTemp = 190 °C	83	[110]
Nitrogen stripping	Xylose	Solvent = H_2O:tolueneCatalyst = Amberlyst-70	N_2 flowrate = 150 mL min^{-1}Time = 200 minTemp = 175 °C	70	[43]
CO_2 stripping	Xylose	Solvent = H_2OCatalyst = Amberlyst-70	CO_2 flowrate = 3.77 g min^{-1}Time = 16 hTemp = 150 °C	52.3	[35]
	Xylose	Solvent = H2O:THF/MIBK	Time = 60 minTemp = 180 °C	56.6	[114]
	Xylose	Solvent = H_2O:CPMECatalyst = Formic acid	CO_2 flowrate = 5 g min^{-1}Temp = 140 °C Time = 300 min	68	[115]
Microwave-assisted heating	Xylose	Solvent = H_2O:CPMECatalyst = sulfonated carbon-based	Temp = 190 °C Time = 60 min	60	[119]
	Xylose	Solvent = H_2OCatalyst = sulfated zirconia on cordierite	Temp = 210 °C Time = 2 min	41	[103]
	Xylose	Solvent = H_2O:CPMECatalyst = Sulphonated nano-sized diamond powder	Temp = 200 °C Time = 50 min	76	[127]
	Xylose	Solvent = H_2O:tolueneCatalyst = H_2SO_4	Temp = 200 °C Time = 20 min	80	[124]
Ultrasound energy	Oil palm fronds	Solvent = ChCl-oxalic acid	Amplitude = 80 %, 3 min (pre-treatment)Temp = 120 °C Time = 60 min	56.5	[128]
	Grass	Solvent = Catalyst = HNO_3	Amplitude = 50 %Temp = 30 °C Time = 60 min	7.24	[120]
Non-conventional reactor	Xylose	Solvent = H_2O:toluene	Temp = 190 °C Time = 2.5 minMillireactor	56	[129]
	Xylose	Catalyst = Formic acid: $AlCl_3$	Temp = 180 °C Time = 15 minmicroreactor	92.2	[70]
	Xylose	Solvent = H_2OCatalyst = H_2SO_4	Temp = 160 °C Time = 10 hVaporization reactor	82.3	[130]
	Xylose	Solvent = H_2OCatalyst = $CrCl_3$:DOWEX@	Temp = 140 °C Time = 10 hMixed matrix membrane reactor	41.1	[131]
	Xylose	Solvent = H_2OCatalyst = SO_4^{2-} : Y −Al_2O_3 and HND-580	CO_2 flowrate = 30 mL/minTemp = 170 °C Time = 1.6 minMicropacked bed reactor	44.65	[132]
	Xylose	Solvent = H_2O:MIBKCatalyst = HCl, NaCl	Temp = 180 °C Time = 4 minSlug flow microreactor	93	[133]

[135]. The conventional Quaker's process was compared to the four investigated processes for the selection of the best alternative while considering the environmental, economic, and safety issues using total annual cost (TAC) as a key economic indicator, Eco-indicator (E199) to quantify the environmental impact and individual risk (IR) to estimate the potential process risk. Their result indicates a constant value for TAC and E199 for all investigated sequences. This was attributed to column A1 (Fig. 10), which contributes most of these indexes due to the high energy requirement for the separation of water present in the feed mixture (90 wt%), making it almost impossible to improve the energy, E199, and TAC indexes in all investigated sequences. HIC shows the highest inherent individual risk due to the inclusion of extra units and compressors which further increases its risk. As summarized in Table 7, the intensified TEC was recommended as the overall best alternative with the lowest individual risk, making it a safer process and slightly cheaper in terms of its TAC as compared to other investigated sequences (TCC, DWCC, and HIC). Although TAC seems economical, the annual cost saving is relatively low (about 12 % using Quaker's process as the benchmark.

The homogeneous azeotrope formed between furfural and water makes it extremely difficult and expensive to be separated by simple distillation. Nhien et al. proposed a hybrid extraction and distillation configuration for furfural purification by screening ten different potential solvents (toluene, benzene, p-xylene, n-octyl acetate, n-decane, cyclohexane, 1-hexene, cyclohexene, cumene and n-butyl chloride) on the bases of their equilibrium distribution coefficient, specific selectivity towards furfural, ease of recovery and economic feasibility [136]. The selected solvents and the feed were investigated for azeotrope formation to examine the ease of separation. Amongst the investigated solvents, p-xylene, n-decane, and cumene were forgone due to forming a homogenous azeotrope with furfural. Also, it was reported that n-octyl acetate produced a tremendous amount of water (600 kg/h of water when feeding: solvent is 1:1), forming a heterogenous azeotrope between furfural, water, and n-octyl-acetate making it unfit.Toluene, benzene, and butyl chloride were selected for the process design due to their suitability. Fig. 11 illustrates the process flow diagram and key design parameters for the three selected solvents. Benzene demonstrated superior extracting affinity for furfural from the feed mixture and the lowest TAC. However, n-butyl chloride was proposed as an extracting solvent in the hybrid purification of furfural production as benzene is a human carcinogen.

Table 7
Comparison of different performance indexes of furfural production.

Process configuration	TAC (US k$/yr.)	Energy consumption (kW)	Equipment cost (million$)	Furfural purity (wt. %)
Quaker oats	9334	20322.97	2.307	99.24
[a]TEC	9075	19973.32	2.5965	99.38
[b]DWCC	9255	20160.11	3.5795	99.7
[c]TCC	9301	20454	2.7712	99.9
[d]HIC	9384	20495.19	2.3791	99.9
[e]HED-Benzene	2118	7161	1.544	99.5
[e]HED-Toluene	7386	29107	3.709	99.5
[e]HED-n-Butyl chloride	4084	16064	2.337	99.5

[a] Thermodynamic equivalent configuration
[b] Divided wall column, [c]Thermocouple configuration
[d] Heat integrated configuration
[e] Hybrid extraction and distillation configuration

While employing a hybrid liquid–liquid extraction and distillation configuration appears to be an intriguing alternative in terms of energy demand, selecting an effective solvent and designing a solvent recovery system remains difficult as it requires experimentally determined interaction parameters. A more sustainable approach toward solvent selection would involve using computational tools such as the COSMO-RS, a quantum chemistry-based method that allows for the prediction of key thermodynamic properties such as solubilities, activity coefficients, partition coefficients, or liquid–liquid equilibria and gas–liquid equilibria solely from the structure of chemicals. This method eliminates the need for a large experimental matrix. It has been widely used for the selection of appropriate solvents for biphasic systems and was recently reviewed by Esteban et al., [137]. It has also been proven to be effective

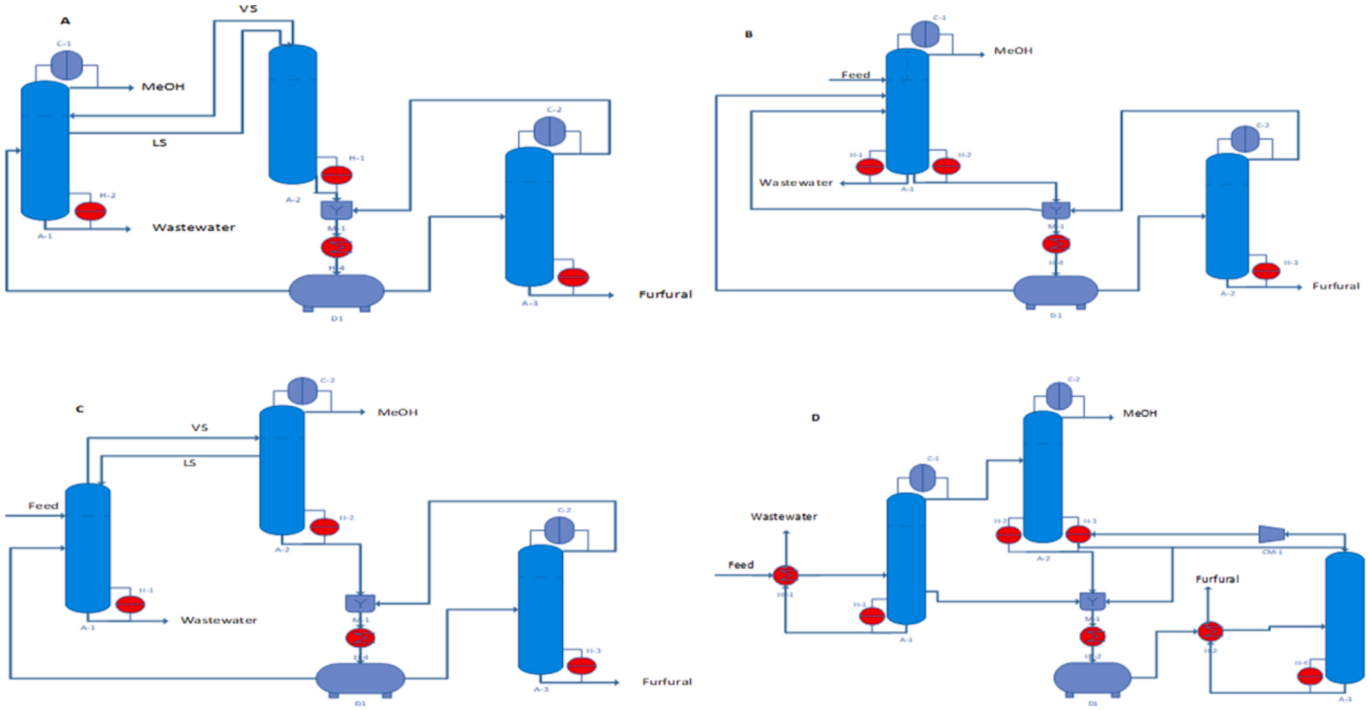

Fig. 10. Process flow diagram for furfural purification using (A) – Thermodynamic equivalent configuration (TEC), (B) – Divided wall column configuration (DWCC), (C) – Thermally coupled configuration (TCC), D – Heat integrated configuration (HIC).

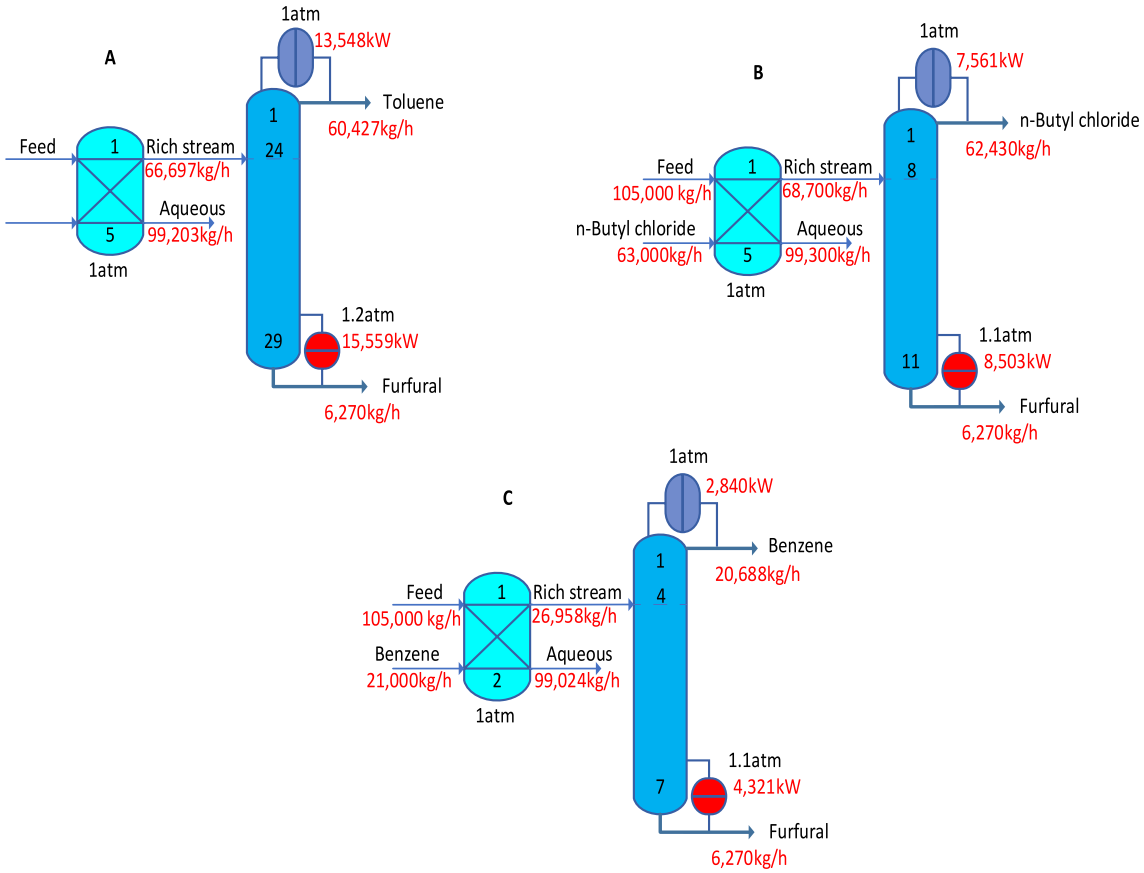

Fig. 11. Hybrid Extraction and Distillation process for furfural purification using (A) – Toluene, (B) – n-Butyl chloride, and (C) – Benzene as an extractive solvent.

within a wide spectrum of studies such as the screening of solvents for furfural production in a biphasic system [61] and in situ extraction of furans [137]. However, no studies have reported its applicability to the furfural purification process.

For this reason, we demonstrate the possibility of designing a hybrid extraction-distillation process for furfural purification through a systematic solvent selection method using the COSMO-RS. Very few extractive solvents have been proposed for furfural purification via liquid–liquid extraction in the literature. Based on this, 76 potential solvents were screened for the liquid–liquid extraction of furfural. The procedure for screening and criteria for selection is summarized in Fig. 12. It consists of the following steps:

i. To ensure the potential solvents are immiscible with water and do not form an azeotrope, binary LLE are estimated using the COMO-RS method by checking for the presence of a miscibility gap for each solvent in water. Solvents showing miscibility gap behavior are selected or otherwise, discarded.
ii. Solvents showing miscibility gap behavior are further screened. Using COSMO-RS method to estimate the activity coefficients of furfural at infinite dilution ($\gamma\infty$) in each solvent as a measure of their ability to selectively separate furfural in a feed mixture. Lower activity coefficients of furfural at infinite dilution indicate higher furfural solubilities in the solvents and thus, higher extraction yields.
iii. The activity coefficient of furfural at infinite dilution in MIBK (the most utilized solvent for biphasic and in situ furfural extraction according to the literature [160]) was set as a threshold. Activity coefficient values of furfural in solvents higher than the set point are discarded as depicted in Fig. S1.
iv. For further assessment of candidates who pass the previous screening, COSMO-RS predicts the partition coefficient log(P). Solvents with higher log(P) values than the threshold (MIBK) are selected, while those with lower log(P) values are discarded. Fig. S2 shows the plot.
v. A constraint was assumed to ensure the selected solvents are easily recovered with less energy requirement and to ease separation via distillation. In this case, the boiling point difference between furfural and the selected solvent must be greater than 20 but less than 60 °C.
vi. Finally, top-performing solvents are ranked based on the CHEM21 solvent selection guide. Top-ranked solvents are thus employed for process simulation and evaluation.

To gain a better understanding of the solvent's interactions and for a fair comparison, the best promising solvents were used to eventually design and optimize the purification process using Aspen Hysys V12.

The feed composition and product specifications can be found in Table S2. To achieve a 99.5 % weight recovery of furfural through the extractor, with 99.0 % and 99.9 % weight recovery of furfural and solvent via distillation, the feed-solvent ratio was adjusted. Only 20,000 kg of GVL was required to obtain the specified product purity while saving up to 82.03 % energy requirement when compared to the conventional Quaker oats process. This can be attributed to the strong interaction of GVL with furfural as can be observed by the COSMO-RS generated σ-profiles as seen in Fig. S3. While the process looks promising, more studies are required to better understand the environmental impact and its overall cost implication.

As our energy and chemical needs increase, it is essential to develop safer, sustainable, and more economical processes that utilize environmentally friendly and non-toxic solvents such as GVL. Herein, we propose a novel process for furfural production directly from lignocellulosic biomass, which is solely based on the utilization of green solvents and solid acid catalysts contrary to conventional industrial processes. The

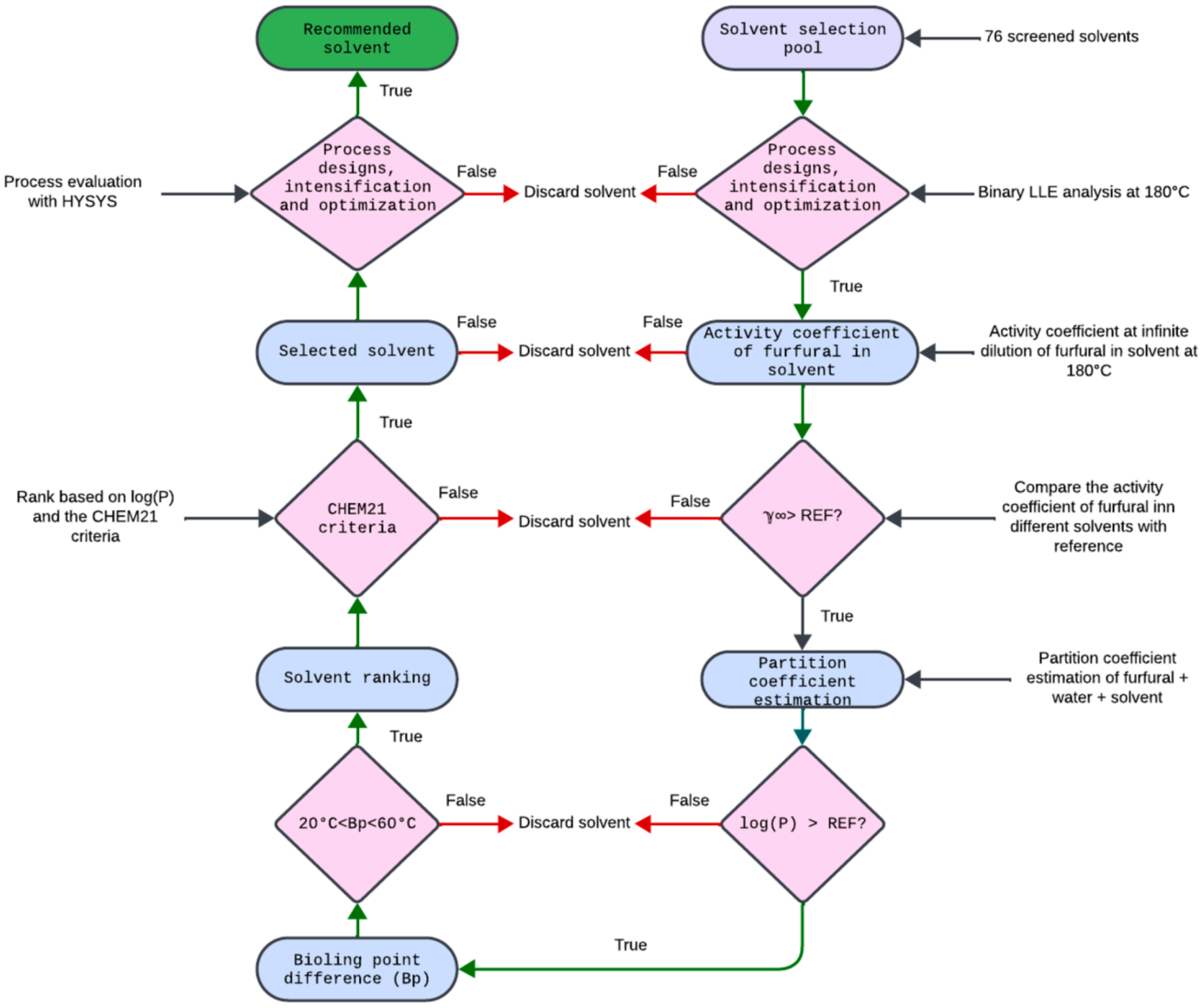

Fig. 12. Algorithm for the screening and selection of solvent for liquid–liquid extraction of furfural.

proposed process begins with a selective catalytic hydrothermal pretreatment and transformation of LCB into pentoses using a solid acid catalyst instead of conventional mineral acid hydrolysis while prioritizing the environmental, safety, and economic issues. These solid acid catalysts can be recovered, reactivated, and recycled back into the process. Solid acid catalysts such as $SO_4^{2-}/TiO^{2-}ZrO_2/La^3$, SC-CCA, Amberlyst-15, $H_3PW_{12}O_{40}$, and many more have been reported to be effective [45,102,138]. Other high-value polymers, such as cellulose and lignin can be recovered from this process and further transformed into platform molecules. The hydrolyzed pentoses are subsequently dehydrated by a solid acid catalyst. In Table 2, we presented varieties of heterogenous solid catalysts that have been reported to effectively dehydrate pentose into furfural with yield as high as 98 %. While most of these studies utilize petro-based solvents, our proposed process seeks to employ water-immersible green solvents such as Gamma-valerolactone. These solvents can selectively extract furfural from the reactive aqueous phase, thus preventing it from further degradation reaction. These solvents can also be recovered and recycled back into the process. Furthermore, The proposed process seeks to reduce the energy requirement during the furfural separation and purification process by utilizing a hybrid liquid–liquid extraction distillation configuration rather than the conventional steam stripping-azeotropic distillation configuration as illustrated in Fig. 13. This approach not only aligns with green chemistry principles but also offers potential economic advantages by reducing energy consumption and enabling the recovery and reusability of key materials.

6. Summary and future prospect

For several decades, the production of furfural from lignocellulosic biomass has been industrialized. By the integration of continuous processing and efficient energy management systems, more modern industrial processes such as the Biofine Process and the Rosenlew continuous process have improved the overall process and product efficiency. The disadvantages of using mineral acid as a catalyst in industrial processes include the formation of acidic wastes and equipment corrosion, besides the high cost of separation and purification of the product. Despite all these challenges, this increasing demand for bio-based chemicals has continued to give reasons for the increase in the industrial-scale production of furfural.

Diverse methodologies emphasize the advancement of laboratory technologies aimed at enhancing furfural production by optimizing yield and diminishing energy usage while concurrently lessening environmental repercussions. The pertinent technologies, typically implemented on a laboratory scale, utilize heterogeneous catalysts rather than mineral acids; in the majority of instances, this facilitates the straightforward separation of the product from the catalyst, mitigates issues related to corrosion, and enables the catalyst's reuse. A range of solid

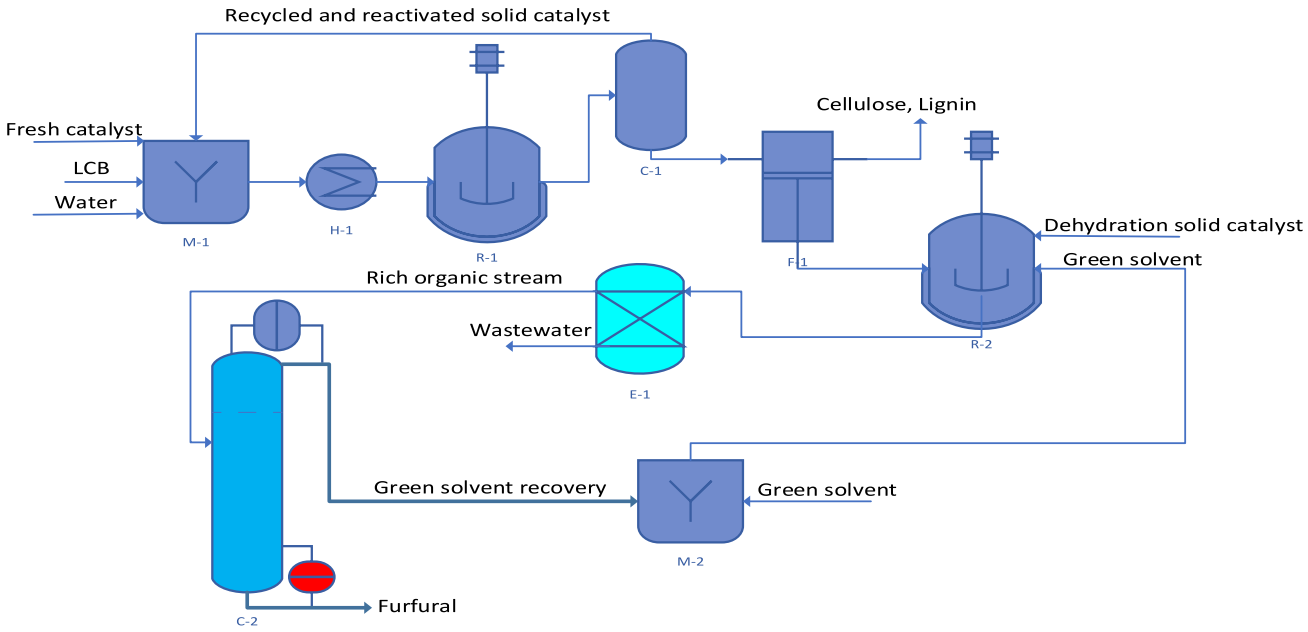

Fig. 13. Proposed Process for furfural production from Lignocellulosic biomass. M−1, M−2 = Mixer, H-1 = Heater, R-1 = Hydrothermal pretreament reactor, R-2 = Dehydration reactor, C-1 = Catalyst recovery and activation system, C-2 = Distillation column, F-1 = Separator, E = Liquid-liquid extraction system.

acid catalysts, including zeolites, ion exchange resins, and metal oxides, have demonstrated enhanced selectivity for furfural production while producing fewer by-products in meticulously regulated laboratory environments under ideal conditions.

Alongside microwave-assisted heating, research is presently focused on various processes in the laboratory, including reactive extraction and the use of environmentally friendly solvents such as ionic liquids and deep eutectic solvents, to improve these techniques. These technologies have great potential to reduce reaction times drastically, increase furfural yields, and save energy compared to conventional heating and solvent-based processes. For instance, microwave-assisted methods have achieved furfural yields as high as 80 % within 20 min in compact biphasic systems, far better than those yields achieved from industrial processes.

Nevertheless, most of these approaches at the laboratory level are in their developing stages and face numerous challenges in reaching commercialization. One of the key issues relates to process scalability. In particular, while heterogeneous catalysts bring about a number of advantages, scaling up catalyst preparation without losing consistent performance and reducing mass transfer limitations when moving to larger reactors are significant challenges. High costs for green solvents and the development of effective systems for solvent recovery, therefore, pose a real barrier that must be overcome before this technology finds a commercialization route.

These technologies, grown in a laboratory environment, hold immense potential for commercialization and can change the game in the furfural industry. As the demand for sustainability and adherence to green chemistry principles escalates, methodologies that promote waste minimization, energy efficiency, and diminished environmental consequences will become critically important. If the problems of scalability, process cost, and stability are overcome, then the various innovations at the laboratory scale could be scaled up to enable the next generation of industrial production of furfural with better yields, short reaction time, and lower cost but with minimal environmental impact. Further commercialization attempts should focus on the integration of these newer technologies into current production schemes, carrying out optimization of reactor design, besides the formulation of economical catalysts and solvents. Knowing that there is a demand for bio-based chemicals, and with the thrust for sustainable industry, a successful transfer from the laboratory into commercial systems could transform the furfural production sector.

7. Conclusion

Significant efforts have been made over the last decade on the sustainable transformation of lignocellulosic biomass into a wide spectrum of marketable products. Lignocellulosic biomass is cheap, renewable, and readily available compared to fossil-based feedstock. Thus, more efficient processes must be developed to mitigate our dependency on fossil-based sources and meet the targets set by the European Union on CO_2 emissions. There is no doubt that furfural, a valuable platform molecule solely obtained from lignocellulosic biomass, will be a major contributor to this cause.

Motivated by economic, environmental, and health implications, this review presented a concise overview of the current challenges and advancements in furfural production from lignocellulosic biomass, highlighting the current trend towards developing a more sustainable and eco-friendly process that can be easily adapted into industrial settings. For an economically competitive production of furfural within the lignocellulosic biorefinery concept, several factors must be considered such as feedstock type and logistic chain, catalysts type and reusability, solvent selection with HSE consideration, waste reduction, choice of reactors-separation configuration with minimal energy consumption, etc. Considering the rising demand for furfural, the industry is expected to evolve progressively in the coming decades, thus, sustainable processes and practices must be implemented to transition towards a more sustainable and eco-friendly viable bio-based chemical industry. This will achieve the European Union's sustainable goals and drive innovation in its production sector.

CRediT authorship contribution statement

Daniel Edumujeze: Writing – review & editing,Investigation, Formal analysis. **Marie-Christine Fournier-Salaün:** Writing – review & editing, Supervision, Investigation, Formal analysis. **Sebastien Leveneur:** Writing – review & editing, Supervision, Investigation, Funding acquisition, Formal analysis.

Declaration of competing interest

The authors declare that they have no known competing financial interests or personal relationships that could have appeared to influence the work reported in this paper.

Acknowledgements

The authors thank the Région Normandie and INSA Rouen Normandie for the financial support.

This work was partly done in the framework of PROMETEE project, funded by Rouen Metropole.

Appendix A. Supplementary data

Supplementary data to this article can be found online at https://doi.org/10.1016/j.fuel.2024.133423.

Data availability

Data will be made available on request.

References

[1] Jorqueira DSS, De Lima LF, Moya SF, Vilcocq L, Richard D, Fraga MA, et al. Critical review of furfural and furfuryl alcohol production: Past, present, and future on heterogeneous catalysis. Appl Catal Gen 2023;665:119360. https://doi.org/10.1016/j.apcata.2023.119360.

[2] Al-Battashi HS, Annamalai N, Sivakumar N, Al-Bahry S, Tripathi BN, Nguyen QD, et al. Lignocellulosic biomass (LCB): a potential alternative biorefinery feedstock for polyhydroxyalkanoates production. Rev Environ Sci Biotechnol 2019;18:183–205. https://doi.org/10.1007/s11157-018-09488-4.

[3] Haq I, Qaisar K, Nawaz A, Akram F, Mukhtar H, Zohu X, et al. Advances in valorization of lignocellulosic biomass towards energy generation. Catalysts 2021;11:309. https://doi.org/10.3390/catal11030309.

[4] Chen X, Song S, Li H, Gözaydın G, Yan N. Expanding the boundary of biorefinery: organonitrogen chemicals from biomass. Acc Chem Res 2021;54:1711–22. https://doi.org/10.1021/acs.accounts.0c00842.

[5] Serrano-Ruiz JC, Luque R, Sepúlveda-Escribano A. Transformations of biomass-derived platform molecules: from high added-value chemicals to fuels via aqueous-phase processing. Chem Soc Rev 2011;40:5266. https://doi.org/10.1039/c1cs15131b.

[6] Wang S, Cheng A, Liu F, Zhang J, Xia T, Zeng X, et al. Catalytic conversion network for lignocellulosic biomass valorization: a panoramic view. Ind Chem Mater 2023;1:188–206. https://doi.org/10.1039/D2IM00054G.

[7] Espinoza Pérez AT, Camargo M, Narváez Rincón PC, Alfaro MM. Key challenges and requirements for sustainable and industrialized biorefinery supply chain design and management: a bibliographic analysis. Renew Sustain Energy Rev 2017;69:350–9. https://doi.org/10.1016/j.rser.2016.11.084.

[8] Singh N, Singhania RR, Nigam PS, Dong C-D, Patel AK, Puri M. Global status of lignocellulosic biorefinery: challenges and perspectives. Bioresour Technol 2022;344:126415. https://doi.org/10.1016/j.biortech.2021.126415.

[9] Maity SK. Opportunities, recent trends and challenges of integrated biorefinery: Part I. Renew Sustain Energy Rev 2015;43:1427–45. https://doi.org/10.1016/j.rser.2014.11.092.

[10] Wilson K, Lee AF. Catalyst design for biorefining. Philos Trans R Soc Math Phys Eng Sci 2016;374:20150081. https://doi.org/10.1098/rsta.2015.0081.

[11] Chandel AK, Garlapati VK, Singh AK, Antunes FAF, Da Silva SS. The path forward for lignocellulose biorefineries: bottlenecks, solutions, and perspective on commercialization. Bioresour Technol 2018;264:370–81. https://doi.org/10.1016/j.biortech.2018.06.004.

[12] Werpy T, Petersen G. Top Value Added Chemicals from Biomass: Volume I - Results of Screening for Potential Candidates from Sugars and Synthesis Gas 2004. https://doi.org/10.2172/15008859.

[13] Machado G, Leon S, Santos F, Lourega R, Dullius J, Mollmann ME, et al. Literature review on furfural production from lignocellulosic biomass. Nat Resour 2016;07:115–29. https://doi.org/10.4236/nr.2016.73012.

[14] Yan K, Wu G, Lafleur T, Jarvis C. Production, properties and catalytic hydrogenation of furfural to fuel additives and value-added chemicals. Renew Sustain Energy Rev 2014;38:663–76. https://doi.org/10.1016/j.rser.2014.07.003.

[15] Yan K, Chen A. Efficient hydrogenation of biomass-derived furfural and levulinic acid on the facilely synthesized noble-metal-free Cu–Cr catalyst. Energy 2013;58:357–63. https://doi.org/10.1016/j.energy.2013.05.035.

[16] Natsir TA, Shimazu S. Fuels and fuel additives from furfural derivatives via etherification and formation of methylfurans. Fuel Process Technol 2020;200:106308. https://doi.org/10.1016/j.fuproc.2019.106308.

[17] Eseyin AE, Steele PH. An overview of the applications of furfural and its derivatives. Int J Adv Chem 2015;3(42). https://doi.org/10.14419/ijac.v3i2.5048.

[18] Lee CBTL, Wu TY. A review on solvent systems for furfural production from lignocellulosic biomass. Renew Sustain Energy Rev 2021;137:110172. https://doi.org/10.1016/j.rser.2020.110172.

[19] Dashtban M, Gilbert A, Fatehi P. Production of furfural: overview and challenges. J Sci Technol For Prod Process 2012;2(2012):44–53.

[20] Dulie NW, Woldeyes B, Demsash HD, Jabasingh AS. An insight into the valorization of hemicellulose fraction of biomass into furfural: catalytic conversion and product separation. Waste Biomass Valorization 2021;12:531–52. https://doi.org/10.1007/s12649-020-00946-1.

[21] Hou Q, Qi X, Zhen M, Qian H, Nie Y, Bai C, et al. Biorefinery roadmap based on catalytic production and upgrading 5-hydroxymethylfurfural. Green Chem 2021;23:119–231. https://doi.org/10.1039/D0GC02770G.

[22] Zhu JY, Pan XJ. Woody biomass pretreatment for cellulosic ethanol production: technology and energy consumption evaluation☆. Bioresour Technol 2010;101:4992–5002. https://doi.org/10.1016/j.biortech.2009.11.007.

[23] Yong KJ, Wu TY, Lee CBTL, Lee ZJ, Liu Q, Jahim JM, et al. Furfural production from biomass residues: current technologies, challenges and future prospects. Biomass Bioenergy 2022;161:106458. https://doi.org/10.1016/j.biombioe.2022.106458.

[24] Mittal A, Black SK, Vinzant TB, O'Brien M, Tucker MP, Johnson DK. Production of furfural from process-relevant biomass-derived pentoses in a biphasic reaction system. ACS Sustain Chem Eng 2017;5:5694–701. https://doi.org/10.1021/acssuschemeng.7b00215.

[25] Binder JB, Blank JJ, Cefali AV, Raines RT. Synthesis of furfural from xylose and xylan. ChemSusChem 2010;3:1268–72. https://doi.org/10.1002/cssc.201000181.

[26] Karinen R, Vilonen K, Niemelä M. Biorefining: heterogeneously catalyzed reactions of carbohydrates for the production of furfural and hydroxymethylfurfural. ChemSusChem 2011;4:1002–16. https://doi.org/10.1002/cssc.201000375.

[27] Romo JE, Bollar NV, Zimmermann CJ, Wettstein SG. Conversion of sugars and biomass to furans using heterogeneous catalysts in biphasic solvent systems. ChemCatChem 2018;10:4805–16. https://doi.org/10.1002/cctc.201800926.

[28] Ennaert T, Van Aelst J, Dijkmans J, De Clercq R, Schutyser W, Dusselier M, et al. Potential and challenges of zeolite chemistry in the catalytic conversion of biomass. Chem Soc Rev 2016;45:584–611. https://doi.org/10.1039/C5CS00859J.

[29] Agirrezabal-Telleria I, Gandarias I, Arias PL. Heterogeneous acid-catalysts for the production of furan-derived compounds (furfural and hydroxymethylfurfural) from renewable carbohydrates: a review. Catal Today 2014;234:42–58. https://doi.org/10.1016/j.cattod.2013.11.027.

[30] Bruce SM, Zong Z, Chatzidimitriou A, Avci LE, Bond JQ, Carreon MA, et al. Small pore zeolite catalysts for furfural synthesis from xylose and switchgrass in a γ-valerolactone/water solvent. J Mol Catal Chem 2016;422:18–22. https://doi.org/10.1016/j.molcata.2016.02.025.

[31] Song W, Liu H, Zhang J, Sun Y, Peng L. Understanding Hβ zeolite in 1,4-dioxane efficiently converts hemicellulose-related sugars to furfural. ACS Catal 2022;12:12833–44. https://doi.org/10.1021/acscatal.2c03227.

[32] Gupta A, Nandanwar SU, Niphadkar P, Simakova I, Bokade V. Maximization of furanic compounds formation by dehydration and hydrogenation of xylose in one step over SO3–H functionalized H-β catalyst in alcohol media. Biomass Bioenergy 2020;139:105646. https://doi.org/10.1016/j.biombioe.2020.105646.

[33] Chizallet C, Bouchy C, Larmier K, Pirngruber G. Molecular views on mechanisms of brønsted acid-catalyzed reactions in zeolites. Chem Rev 2023;123:6107–96. https://doi.org/10.1021/acs.chemrev.2c00896.

[34] Wang Y, Dai Y, Wang T, Li M, Zhu Y, Zhang L. Efficient conversion of xylose to furfural over modified zeolite in the recyclable water/n-butanol system. Fuel Process Technol 2022;237:107472. https://doi.org/10.1016/j.fuproc.2022.107472.

[35] Sato O. Effect of extraction on furfural production by solid acid-catalyzed xylose dehydration in water. J Supercrit Fluids 2019.

[36] Le Guenic S, Gergela D, Ceballos C, Delbecq F, Len C. Furfural production from d-xylose and xylan by using stable nafion NR50 and NaCl in a microwave-assisted biphasic reaction. Molecules 2016;21:1102. https://doi.org/10.3390/molecules21081102.

[37] Mittal A, Ruddy DA, Chen X, Johnson DK. Simultaneous dehydration of glucose and xylose present in a process-relevant biorefinery hydrolysate to furfurals using heterogeneous solid acid catalysts. Energy Fuels 2023;37:13115–25. https://doi.org/10.1021/acs.energyfuels.3c01597.

[38] Mishra RK, Kumar VB, Victor A, Pulidindi IN, Gedanken A. Selective production of furfural from the dehydration of xylose using Zn doped CuO catalyst. Ultrason Sonochem 2019;56:55–62. https://doi.org/10.1016/j.ultsonch.2019.03.015.

[39] Bhaumik P, Dhepe PL. From lignocellulosic biomass to furfural: insight into the active species of a silica-supported tungsten oxide catalyst. ChemCatChem 2017;9:2709–16. https://doi.org/10.1002/cctc.201600784.

[40] Moreno-Marrodan C, Barbaro P, Caporali S, Bossola F. Low-temperature continuous-flow dehydration of xylose over water-tolerant niobia-titania heterogeneous catalysts. ChemSusChem 2018;11:3649–60. https://doi.org/10.1002/cssc.201801414.

[41] Zhang L, Xi G, Yu K, Yu H, Wang X. Furfural production from biomass–derived carbohydrates and lignocellulosic residues via heterogeneous acid catalysts. Ind Crops Prod 2017;98:68–75. https://doi.org/10.1016/j.indcrop.2017.01.014.

[42] Lu Y, He Q, Peng Q, Chen W, Cheng Q, Song G, et al. Directional synthesis of furfural compounds from holocellulose catalyzed by sulfamic acid. Cellul 2021; 28:8343–54. https://doi.org/10.1007/s10570-021-04070-8.

[43] Agirrezabal-Telleria I, Larreategui A, Requies J, Güemez MB, Arias PL. Furfural production from xylose using sulfonic ion-exchange resins (Amberlyst) and simultaneous stripping with nitrogen. Bioresour Technol 2011;102:7478–85. https://doi.org/10.1016/j.biortech.2011.05.015.

[44] Teng X, Si Z, Li S, Yang Y, Wang Z, Li G, et al. Tin-loaded sulfonated rape pollen for efficient catalytic production of furfural from corn stover. Ind Crops Prod 2020;151:112481. https://doi.org/10.1016/j.indcrop.2020.112481.

[45] Zhang L, Xi G, Zhang J, Yu H, Wang X. Efficient catalytic system for the direct transformation of lignocellulosic biomass to furfural and 5-hydroxymethylfurfural. Bioresour Technol 2017;224:656–61. https://doi.org/10.1016/j.biortech.2016.11.097.

[46] Shuai L, Luterbacher J. Organic solvent effects in biomass conversion reactions. ChemSusChem 2016;9:133–55. https://doi.org/10.1002/cssc.201501148.

[47] Chen Z, Bai X, A L, Wan C. High-solid lignocellulose processing enabled by natural deep eutectic solvent for lignin extraction and industrially relevant production of renewable chemicals. ACS Sustain Chem Eng 2018;6:12205–16. https://doi.org/10.1021/acssuschemeng.8b02541.

[48] Li X, Liu Q, Luo C, Gu X, Lu L, Lu X. Kinetics of furfural production from corn cob in γ-valerolactone using dilute sulfuric acid as catalyst. ACS Sustain Chem Eng 2017;5:8587–93. https://doi.org/10.1021/acssuschemeng.7b00950.

[49] Hu X, Westerhof RJM, Dong D, Wu L, Li C-Z. Acid-catalyzed conversion of xylose in 20 solvents: insight into interactions of the solvents with xylose, furfural, and the acid catalyst. ACS Sustain Chem Eng 2014;2:2562–75. https://doi.org/10.1021/sc5004659.

[50] Mellmer MA, Sener C, Gallo JMR, Luterbacher JS, Alonso DM, Dumesic JA. Solvent effects in acid-catalyzed biomass conversion reactions. Angew Chem 2014;126:12066–9. https://doi.org/10.1002/ange.201408359.

[51] Grisel RJH, Van Der Waal JC, De Jong E, Huijgen WJJ. Acid catalysed alcoholysis of wheat straw: towards second generation furan-derivatives. Catal Today 2014; 223:3–10. https://doi.org/10.1016/j.cattod.2013.07.008.

[52] Yong T-L-K, Mohamad N, Yusof NNM. Furfural production from oil palm biomass using a biomass-derived supercritical ethanol solvent and formic acid catalyst. Procedia Eng 2016;148:392–400. https://doi.org/10.1016/j.proeng.2016.06.495.

[53] Ye L, Han Y, Wang X, Lu X, Qi X, Yu H. Recent progress in furfural production from hemicellulose and its derivatives: conversion mechanism, catalytic system, solvent selection. Mol Catal 2021;515:111899. https://doi.org/10.1016/j.mcat.2021.111899.

[54] Lin H, Chen J, Zhao Y, Wang S. Conversion of C5 carbohydrates into furfural catalyzed by SO3H-functionalized ionic liquid in renewable γ-valerolactone. Energy Fuels 2017.

[55] Liu P. Efficient conversion of xylan and rice husk to furfural over immobilized imidazolium acidic ionic liquids. React Kinet 2022.

[56] Matsagar BM, Hossain SA, Islam T, Alamri HR, Alothman ZA, Yamauchi Y, et al. Direct production of furfural in one-pot fashion from raw biomass using brønsted acidic ionic liquids. Sci Rep 2017;7:13508. https://doi.org/10.1038/s41598-017-13946-4.

[57] Penín L, López M, Santos V, Parajó JC. Evaluation of Acidic Ionic Liquids as Catalysts for Furfural Production from Eucalyptus nitens Wood 2022.

[58] Nis B. Efficient direct conversion of lignocellulosic biomass into biobased platform chemicals in ionic liquid-water medium. Renew. Energy 2021.

[59] Peleteiro S, Santos V, Garrote G, Parajó JC. Furfural production from eucalyptus wood using an acidic ionic liquid. Carbohydr Polym 2016;146:20–5. https://doi.org/10.1016/j.carbpol.2016.03.049.

[60] Peleteiro S, Da Costa Lopes AM, Garrote G, Bogel-Łukasik R, Parajó JC. Manufacture of furfural in biphasic media made up of an ionic liquid and a co-solvent. Ind Crops Prod 2015;77:163–6. https://doi.org/10.1016/j.indcrop.2015.08.048.

[61] Cañada-Barcala A, Rodríguez-Llorente D, López L, Navarro P, Hernández E, Águeda VI, et al. Sustainable production of furfural in biphasic reactors using terpenoids and hydrophobic eutectic solvents. ACS Sustain Chem Eng 2021;9: 10266–75. https://doi.org/10.1021/acssuschemeng.1c02798.

[62] Carvalho AV, Da Costa Lopes AM, Bogel-Łukasik R. Relevance of the acidic 1-butyl-3-methylimidazolium hydrogen sulphate ionic liquid in the selective catalysis of the biomass hemicellulose fraction. RSC Adv 2015;5:47153–64. https://doi.org/10.1039/C5RA07159C.

[63] Liu C-Z, Wang F, Stiles AR, Guo C. Ionic liquids for biofuel production: opportunities and challenges. Appl Energy 2012;92:406–14. https://doi.org/10.1016/j.apenergy.2011.11.031.

[64] Sen SM, Binder JB, Raines RT, Maravelias CT. Conversion of biomass to sugars via ionic liquid hydrolysis: process synthesis and economic evaluation. Biofuels Bioprod Biorefining 2012;6:444–52. https://doi.org/10.1002/bbb.1336.

[65] Liu P, Shi S, Wei R, Gao L, Zhang J, Xiao G. Dehydration of xylose and xylan to furfural using P-Zr-SBA-15 catalyst in aqueous or biphasic system. ChemistrySelect 2023;8:e202300902.

[66] Rusanen A, Lappalainen K, Kärkkäinen J, Lassi U. Furfural and 5-hydroxymethylfurfural production from sugar mixture using deep eutectic solvent/MIBK system. ChemistryOpen 2021;10:1004–12. https://doi.org/10.1002/open.202100163.

[67] Kim TH. Low acid hydrothermal fractionation of Giant Miscanthus for production of xylose-rich hydrolysate and furfural. Bioresour Technol 2016.

[68] Deng A, Ren J, Li H, Peng F, Sun R. Corncob lignocellulose for the production of furfural by hydrothermal pretreatment and heterogeneous catalytic process. RSC Adv 2015;5:60264–72. https://doi.org/10.1039/C5RA10472F.

[69] Raman JK, Gnansounou E. Furfural production from empty fruit bunch – a biorefinery approach. Ind Crops Prod 2015;69:371–7. https://doi.org/10.1016/j.indcrop.2015.02.063.

[70] Tongtummachat T, Jaree A, Akkarawatkhoosith N. Continuous hydrothermal furfural production from xylose in a microreactor with dual-acid catalysts. RSC Adv 2022;12:23366–78. https://doi.org/10.1039/D2RA03609F.

[71] Zhang S, Lu J, Li M, Cai Q. Efficient production of furfural from corncob by an integrated mineral-organic-lewis acid catalytic process. BioResources 2017;12 (2965–81).

[72] Li W, Zhu Y, Lu Y, Liu Q, Guan S, Chang H, et al. Enhanced furfural production from raw corn stover employing a novel heterogeneous acid catalyst. Bioresour Technol 2017;245:258–65. https://doi.org/10.1016/j.biortech.2017.08.077.

[73] Xu Z, Li W, Du Z, Wu H, Jameel H, Chang H, et al. Conversion of corn stalk into furfural using a novel heterogeneous strong acid catalyst in γ-valerolactone. Bioresour Technol 2015;198:764–71. https://doi.org/10.1016/j.biortech.2015.09.104.

[74] Nie Y, Hou Q, Li W, Bai C, Bai X, Ju M. Efficient synthesis of furfural from biomass using sncl4 as catalyst in ionic liquid. Molecules 2019;24:594. https://doi.org/10.3390/molecules24030594.

[75] Zhang L. Conversion of xylan, d-xylose and lignocellulosic biomass into furfural using AlCl3 as catalyst in ionic liquid. Bioresour Technol 2013.

[76] Lee CBTL, Wu TY, Ting CH, Tan JK, Siow LF, Cheng CK, et al. One-pot furfural production using choline chloride-dicarboxylic acid based deep eutectic solvents under mild conditions. Bioresour Technol 2019;278:486–9. https://doi.org/10.1016/j.biortech.2018.12.034.

[77] Da Silva LV, López-Sotelo JB, Correa-Guimarães A, Hernández-Navarro S, Sánchez-Bascones M, Navas-Gracia LM, et al. A kinetic study on microwave-assisted conversion of cellulose and lignocellulosic waste into hydroxymethylfurfural/furfural. Bioresour Technol 2015;180:88–96. https://doi.org/10.1016/j.biortech.2014.12.089.

[78] Taherzadeh MJ, Karimi K. Pretreatment of lignocellulosic wastes to improve ethanol and biogas production: a review. Int J Mol Sci 2008.

[79] Gómez Millán G, Phiri J, Mäkelä M, Maloney T, Balu AM, Pineda A, et al. Furfural production in a biphasic system using a carbonaceous solid acid catalyst. Appl Catal Gen 2019;585:117180. https://doi.org/10.1016/j.apcata.2019.117180.

[80] Wang X, Zhang C, Lin Q, Cheng B, Kong F, Li H, et al. Solid acid-induced hydrothermal treatment of bagasse for production of furfural and levulinic acid by a two-step process. Ind Crops Prod 2018;123:118–27. https://doi.org/10.1016/j.indcrop.2018.06.064.

[81] Wang Q, Zhuang X, Wang W, Tan X, Yu Q, Qi W, et al. Rapid and simultaneous production of furfural and cellulose-rich residue from sugarcane bagasse using a pressurized phosphoric acid-acetone-water system. Chem Eng J 2018;334: 698–706. https://doi.org/10.1016/j.cej.2017.10.089.

[82] Li C, Ding D, Xia Q, Liu X, Wang Y. Conversion of raw lignocellulosic biomass into branched long-chain alkanes through three tandem steps. ChemSusChem 2016;9: 1712–8. https://doi.org/10.1002/cssc.201600386.

[83] Luo Y, Li Z, Zuo Y, Su Z, Hu C. A simple two-step method for the selective conversion of hemicellulose in *pubescens* to furfural. ACS Sustain Chem Eng 2017; 5:8137–47. https://doi.org/10.1021/acssuschemeng.7b01766.

[84] IARC Working Group on the Evaluation of Carcinogenic Risks to Humans, World Health Organization, International Agency for Research on Cancer, editors. Some chemicals present in industrial and consumer products, food and drinking-water. Lyon: IARC Press; 2013.

[85] Prat D, Wells A, Hayler J, Sneddon H, McElroy CR, Abou-Shehada S, et al. CHEM21 selection guide of classical- and less classical-solvents. Green Chem 2016;18:288–96. https://doi.org/10.1039/C5GC01008J.

[86] Bharti A, Banerjee T. Enhancement of bio-oil derived chemicals in aqueous phase using ionic liquids: experimental and COSMO-SAC predictions using a modified hydrogen bonding expression. Fluid Phase Equilib 2015;400:27–37. https://doi.org/10.1016/j.fluid.2015.04.029.

[87] Rakić E, Kostyniuk A, Nikačević N, Likozar B. Reaction microkinetic model of xylose dehydration to furfural over beta zeolite catalyst. Biomass Convers Biorefinery 2023. https://doi.org/10.1007/s13399-023-04969-1.

[88] Jing Q, Lü X. Kinetics of non-catalyzed decomposition of D-xylose in high temperature liquid water. Chin J Chem Eng 2007;15:666–9. https://doi.org/10.1016/S1004-9541(07)60143-8.

[89] Dunlop AP. Furfural formation and behavior. Ind Eng Chem 1948;40:204–9. https://doi.org/10.1021/ie50458a006.

[90] Chen Z, Zhang W, Xu J, Li P. Kinetics of xylose dehydration into furfural in acetic acid. Chin J Chem Eng 2015;23:659–66. https://doi.org/10.1016/j.cjche.2013.08.003.

[91] Krzelj V, Ferreira Liberal J, Papaioannou M, Van Der Schaaf J, Neira d'Angelo MF. Kinetic model of xylose dehydration for a wide range of sulfuric acid concentrations. Ind Eng Chem Res 2020;59:11991–2003. https://doi.org/10.1021/acs.iecr.0c01197.

[92] Marcotullio G, De Jong W. Chloride ions enhance furfural formation from d-xylose in dilute aqueous acidic solutions. Green Chem 2010;12:1739. https://doi.org/10.1039/b927424c.

[93] Choudhary V, Pinar AB, Sandler SI, Vlachos DG, Lobo RF. Xylose isomerization to xylulose and its dehydration to furfural in aqueous media. ACS Catal 2011;1: 1724–8. https://doi.org/10.1021/cs200461t.

[94] Ershova O, Kanervo J, Hellsten S, Sixta H. The role of xylulose as an intermediate in xylose conversion to furfural: insights via experiments and kinetic modelling. RSC Adv 2015;5:66727–37. https://doi.org/10.1039/C5RA10855A.
[95] Nabarlatz D, Farriol X, Montané D. Kinetic modeling of the autohydrolysis of lignocellulosic biomass for the production of hemicellulose-derived oligosaccharides. Ind Eng Chem Res 2004;43:4124–31. https://doi.org/10.1021/ie034238i.
[96] Brownlee HJ, Miner CS. Industrial development of furfural. Ind Eng Chem 1948; 40:201–4. https://doi.org/10.1021/ie50458a005.
[97] Cai CM, Zhang T, Kumar R, Wyman CE. Integrated furfural production as a renewable fuel and chemical platform from lignocellulosic biomass. J Chem Technol Biotechnol 2014;89:2–10. https://doi.org/10.1002/jctb.4168.
[98] Eifert T, Liauw MA. Process analytical technology (PAT) applied to biomass valorisation: a kinetic study on the multiphase dehydration of xylose to furfural. React Chem Eng 2016;1:521–32. https://doi.org/10.1039/C6RE00082G.
[99] Ogundowo O, Sadanandam G, Ibrahim H. Furfural from flax straw using sulfonated carbonaceous acid catalyst: parametric and kinetic studies. React Kinet Mech Catal 2023;136:2535–54. https://doi.org/10.1007/s11144-023-02466-0.
[100] Danon B, Hongsiri W, Van Der Aa L, De Jong W. Kinetic study on homogeneously catalyzed xylose dehydration to furfural in the presence of arabinose and glucose. Biomass Bioenergy 2014;66:364–70. https://doi.org/10.1016/j.biombioe.2014.04.007.
[101] Li X, Liu Q, Si C, Lu L, Luo C, Gu X, et al. Green and efficient production of furfural from corn cob over H-ZSM-5 using γ-valerolactone as solvent. Ind Crops Prod 2018;120:343–50. https://doi.org/10.1016/j.indcrop.2018.04.065.
[102] Li X, Yang J, Xu R, Lu L, Kong F, Liang M, et al. Kinetic study of furfural production from Eucalyptus sawdust using H-SAPO-34 as solid Brønsted acid and Lewis acid catalysts in biomass-derived solvents. Ind Crops Prod 2019;135: 196–205. https://doi.org/10.1016/j.indcrop.2019.04.047.
[103] Gómez Millán G, El Assal Z, Nieminen K, Hellsten S, Llorca J, Sixta H. Fast furfural formation from xylose using solid acid catalysts assisted by a microwave reactor. Fuel Process Technol 2018;182:56–67. https://doi.org/10.1016/j.fuproc.2018.10.013.
[104] Iglesias J, Melero JA, Morales G, Paniagua M, Hernández B. Dehydration of xylose to furfural in alcohol media in the presence of solid acid catalysts. ChemCatChem 2016;8:2089–99. https://doi.org/10.1002/cctc.201600292.
[105] Sun K, Shao Y, Liu P, Zhang L, Gao G, Dong D, et al. A solid iron salt catalyst for selective conversion of biomass-derived C5 sugars to furfural. Fuel 2021;300: 120990. https://doi.org/10.1016/j.fuel.2021.120990.
[106] Dos Santos Rocha MSR, Pratto B, De Sousa R, Almeida RMRG, Cruz AJGD. A kinetic model for hydrothermal pretreatment of sugarcane straw. Bioresour Technol 2017;228:176–85. https://doi.org/10.1016/j.biortech.2016.12.087.
[107] Köchermann J, Mühlenberg J, Klemm M. Kinetics of hydrothermal furfural production from organosolv hemicellulose and d -xylose. Ind Eng Chem Res 2018; 57:14417–27. https://doi.org/10.1021/acs.iecr.8b03402.
[108] Gadewar SB, Malone MF, Doherty MF. Selectivity targets for batch reactive distillation. Ind Eng Chem Res 2000;39:1565–75. https://doi.org/10.1021/ie990497p.
[109] Metkar PS, Till EJ, Corbin DR, Pereira CJ, Hutchenson KW, Sengupta SK. Reactive distillation process for the production of furfural using solid acid catalysts. Green Chem 2015;17:1453–66. https://doi.org/10.1039/C4GC01912A.
[110] Köchermann J, Klemm M. Hydrothermal reactive distillation of biomass and biomass hydrolysates for the recovery and separation of furfural and its byproducts. Ind Eng Chem Res 2023;62:6886–96. https://doi.org/10.1021/acs.iecr.3c00259.
[111] Krzelj V, Van Kampen J, Van Der Schaaf J, Neira d'Angelo MF. Furfural production by reactive stripping: process optimization by a combined modeling and experimental approach. Ind Eng Chem Res 2019;58:16126–37. https://doi.org/10.1021/acs.iecr.9b00445.
[112] Sangarunlert W, Piumsomboon P, Ngamprasertsith S. Furfural production by acid hydrolysis and supercritical carbon dioxide extraction from rice husk. Korean J Chem Eng 2007;24:936–41. https://doi.org/10.1007/s11814-007-0101-z.
[113] Yamaguchi A, Hiyoshi N, Sato O, Shirai M. Dehydration of triol compounds in high-temperature liquid water under high-pressure carbon dioxide. Top Catal 2010;53:487–91. https://doi.org/10.1007/s11244-010-9476-x.
[114] Morais ARC, Matuchaki MDDJ, Andreaus J, Bogel-Lukasik R. A green and efficient approach to selective conversion of xylose and biomass hemicellulose into furfural in aqueous media using high-pressure CO_2 as a sustainable catalyst. Green Chem 2016;18:2985–94. https://doi.org/10.1039/C6GC00043F.
[115] Namhaed K, Pérès Y, Kiatkittipong W, Triquet T, Camy S, Cognet P. Integrated supercritical carbon dioxide extraction for efficient furfural production from xylose using formic acid as a catalyst. J Supercrit Fluids 2024;210:106274. https://doi.org/10.1016/j.supflu.2024.106274.
[116] Ricciardi L, Verboom W, Lange J-P, Huskens J. Local overheating explains the rate enhancement of xylose dehydration under microwave heating. ACS Sustain Chem Eng 2019;7:14273–9. https://doi.org/10.1021/acssuschemeng.9b03580.
[117] Curet S, Rouaud O, Boillereaux L. Microwave tempering and heating in a single-mode cavity: numerical and experimental investigations. Chem Eng Process Process Intensif 2008;47:1656–65. https://doi.org/10.1016/j.cep.2007.09.011.
[118] Delbecq F, Wang Y, Muralidhara A, El Ouardi K, Marlair G, Len C. Hydrolysis of hemicellulose and derivatives—a review of recent advances in the production of furfural. Front Chem 2018;6:146. https://doi.org/10.3389/fchem.2018.00146.
[119] Wang Y, Delbecq F, Kwapinski W, Len C. Application of sulfonated carbon-based catalyst for the furfural production from d -xylose and xylan in a microwave-assisted biphasic reaction. Mol Catal 2017;438:167–72. https://doi.org/10.1016/j.mcat.2017.05.031.
[120] Bizzi CA, Santos D, Sieben TC, Motta GV, Mello PA, Flores EMM. Furfural production from lignocellulosic biomass by ultrasound-assisted acid hydrolysis. Ultrason Sonochem 2019;51:332–9. https://doi.org/10.1016/j.ultsonch.2018.09.011.
[121] Díaz-Ortiz Á, Prieto P, de la Hoz A. A critical overview on the effect of microwave irradiation in organic synthesis. Chem Rec 2019;19:85–97. https://doi.org/10.1002/tcr.201800059.
[122] Herrero MA, Kremsner JM, Kappe CO. Nonthermal microwave effects revisited: on the importance of internal temperature monitoring and agitation in microwave chemistry. J Org Chem 2008;73:36–47. https://doi.org/10.1021/jo7022697.
[123] Kappe CO. Unraveling the mysteries of microwave chemistry using silicon carbide reactor technology. Acc Chem Res 2013;46:1579–87. https://doi.org/10.1021/ar300318c.
[124] Ricciardi L, Verboom W, Lange J, Huskens J. Reactive extraction enhanced by synergic microwave heating: furfural yield boost in biphasic systems. ChemSusChem 2020;13:3589–93. https://doi.org/10.1002/cssc.202000966.
[125] Sasmal S, Goud VV, Mohanty K. Ultrasound assisted lime pretreatment of lignocellulosic biomass toward bioethanol production. Energy Fuels 2012;26: 3777–84. https://doi.org/10.1021/ef300669w.
[126] Wang S, Li F, Zhang P, Jin S, Tao X, Tang X, et al. Ultrasound assisted alkaline pretreatment to enhance enzymatic saccharification of grass clipping. Energy Convers Manag 2017;149:409–15. https://doi.org/10.1016/j.enconman.2017.07.042.
[127] Delbecq F, Takahashi Y, Kondo T, Corbas CC, Ramos ER, Len C. Microwave assisted efficient furfural production using nano-sized surface-sulfonated diamond powder. Catal Commun 2018;110:74–8. https://doi.org/10.1016/j.catcom.2018.03.020.
[128] Lee CBTL, Wu TY, Cheng CK, Siow LF, Chew IML. Nonsevere furfural production using ultrasonicated oil palm fronds and aqueous choline chloride-oxalic acid. Ind Crops Prod 2021;166:113397. https://doi.org/10.1016/j.indcrop.2021.113397.
[129] Papaioannou M, Kleijwegt RJT, Van Der Schaaf J, Neira d'Angelo MF. Furfural production by continuous reactive extraction in a millireactor under the taylor flow regime. Ind Eng Chem Res 2019;58:16106–15. https://doi.org/10.1021/acs.iecr.9b00604.
[130] Shen T, Hu Y, Hu R, Zhuang W, Li M, Niu H, et al. Continuous production of furfural from pulp prehydrolysate in a vaporization reactor. Ind Crops Prod 2020; 153:112565. https://doi.org/10.1016/j.indcrop.2020.112565.
[131] Jin H, Liu X, Ban Y, Peng Y, Jiao W, Wang P, et al. Conversion of xylose into furfural in a MOF-based mixed matrix membrane reactor. Chem Eng J 2016;305: 12–8. https://doi.org/10.1016/j.cej.2015.10.115.
[132] Lu H-X, Yang W-Y, Shi Y-X, Wang H-B, Mao H, Sang L, et al. Fast and continuous conversion of xylose to furfural in micropacked bed reactors. Chem Eng Sci 2023; 266:118256. https://doi.org/10.1016/j.ces.2022.118256.
[133] Guo W, Bruining HC, Heeres HJ, Yue J. Efficient synthesis of furfural from xylose over HCl catalyst in slug flow microreactors promoted by NaCl addition. AIChE J 2022;68:e17606. https://doi.org/10.1002/aic.17606.
[134] Tafete GA, Habtu NG. Reactor configuration, operations and structural catalyst design in process intensification of catalytic reactors: a review. Chem Eng Process - Process Intensif 2023;184:109290. https://doi.org/10.1016/j.cep.2023.109290.
[135] Contreras-Zarazúa G, Sánchez-Ramírez E, Vázquez-Castillo JA, Ponce-Ortega JM, Errico M, Kiss AA, et al. Inherently safer design and optimization of intensified separation processes for furfural production. Ind Eng Chem Res 2019;58: 6105–20. https://doi.org/10.1021/acs.iecr.8b03646.
[136] Nhien LC, Long NVD, Lee M. Process design of hybrid extraction and distillation processes through a systematic solvent selection for furfural production. Energy Procedia 2017;105:1084–9. https://doi.org/10.1016/j.egypro.2017.03.467.
[137] Esteban J, Vorholt AJ, Leitner W. An overview of the biphasic dehydration of sugars to 5-hydroxymethylfurfural and furfural: a rational selection of solvents using COSMO-RS and selection guides. Green Chem 2020;22:2097–128. https://doi.org/10.1039/C9GC04208C.
[138] Li H, Deng A, Ren J, Liu C, Lu Q, Zhong L, et al. Catalytic hydrothermal pretreatment of corncob into xylose and furfural via solid acid catalyst. Bioresour Technol 2014;158:313–20. https://doi.org/10.1016/j.biortech.2014.02.059.